Features that Govern Terminator Strength in Plants

Sayeh Gorjifard[1], Tobias Jores[1], Jackson Tonnies[1,2], Nicholas A Mueth[1], Kerry Bubb[1], Travis Wrightsman[3], Edward S Buckler[3,4,5], Stanley Fields[1,6], Josh T Cuperus[1], Christine Queitsch[1,7]

[1] Department of Genome Sciences, University of Washington, Seattle, WA 98195.
[2] Graduate Program in Biology, University of Washington, Seattle, WA 98195.
[3] Section of Plant Breeding and Genetics, Cornell University, Ithaca, NY 14853.
[4] Agricultural Research Service, United States Department of Agriculture, Ithaca, NY 14853.
[5] Institute for Genomic Diversity, Cornell University, Ithaca, NY 14853.
[6] Department of Medicine, University of Washington, Seattle, WA 98195.
[7] Corresponding Author: Christine Queitsch, queitsch@uw.edu

ABSTRACT

The 3' end of a gene, often called a terminator, modulates mRNA stability, localization, translation, and polyadenylation. Here, we adapted Plant STARR-seq, a massively parallel reporter assay, to measure the activity of over 50,000 terminators from the plants *Arabidopsis thaliana* and *Zea mays*. We characterize thousands of plant terminators, including many that outperform bacterial terminators commonly used in plants. Terminator activity is species-specific, differing in tobacco leaf and maize protoplast assays. While recapitulating known biology, our results reveal the relative contributions of polyadenylation motifs to terminator strength. We built a computational model to predict terminator strength and used it to conduct *in silico* evolution that generated optimized synthetic terminators. Additionally, we discover alternative polyadenylation sites across tens of thousands of terminators; however, the strongest terminators tend to have a dominant cleavage site. Our results establish features of plant terminator function and identify strong naturally occurring and synthetic terminators.

INTRODUCTION

A critical challenge is producing enough food for a growing world population that is likely to reach over 9 billion people by the year 2050 (Department of Economic and Social Affairs 2022). Food security can be bolstered through crop engineering, which can improve yields and increase tolerance to pathogens and environmental stresses (Hickey et al. 2019; Eshed and Lippman 2019). However, for crop engineering to be successful, precise control over transgene expression is required. In plants, past efforts to optimize critical *cis*-elements have mostly focused on the identification, characterization, and manipulation of upstream regulatory elements such as promoters (Tobias Jores et al. 2021, 2020; Zhou et al. 2023; X. Wang et al. 2021; Rodríguez-Leal et al. 2017). Although these upstream elements can produce large effects on gene expression, other sequence elements also contribute. For example, the 3' end of a gene — commonly called a terminator — contains sequence motifs necessary for mRNA 3' end maturation, cleavage, and polyadenylation (Kumar et al. 2019). Terminators also affect mRNA stability, nuclear export, and translation (Felipe F. de Felippes and Waterhouse 2023). Moreover, terminators play a central role in transgene silencing mediated by small RNAs (Baeg,

Iwakawa, and Tomari 2017; Allen and Howell 2010; Qin et al. 2012; Diamos and Mason 2018; F de Felippes et al. 2020).

Although the choice of terminator significantly impacts transgene expression, only a few terminators — often those derived from viruses or bacteria — are commonly used in crop engineering. These viral or bacterial sequences make transgene silencing more likely (Dadami et al. 2014; Diamos and Mason 2018). Compared to the commonly used *Agrobacterium tumefaciens* nopaline synthase terminator (tNOS), the terminator from the *Arabidopsis thaliana* heat shock protein 18.2 results in increased transgene expression and mRNA stability, and decreased silencing (Nagaya et al. 2010; Hirai et al. 2011; Pérez-González and Caro 2018; F de Felippes et al. 2020; Felipe Fenselau de Felippes, Shand, and Waterhouse 2022). This finding highlights the need to characterize and optimize native plant terminators as building blocks for crop engineering applications (Ingelbrecht et al. 1989; Diamos and Mason 2018; C. Tian et al. 2022).

Plant terminators have been characterized by analysis of wild-type and mutated versions of a handful of terminators, from both plant and non-plant sources, or by searching for motifs enriched in genomic sequences surrounding mRNA cleavage sites. These studies established three main *cis*-acting elements required for 3' end processing (A. G. Hunt 1994; Shen et al. 2008; Loke et al. 2005; Bernardes and Menossi 2020; Felipe F. de Felippes and Waterhouse 2023). The first element is the far upstream element (FUE), which resides in a U-rich region located 30 – 150 nucleotides upstream of the cleavage site and often contains one or more UGUA sequences. The second is the near upstream element (NUE), which resides in an A-rich region located 10 – 30 nucleotides upstream of the cleavage site and contains the polyadenylation signal AAUAAA. The third is the cleavage element (CE), which contains the cleavage site, formed by a UA or CA dinucleotide embedded in a U-rich region. Although the general pattern and nucleotide preferences of *cis*-acting elements in plant terminators are known, their relative contributions to terminator strength and species specificity have not been determined.

Here, we characterized over 50,000 terminators from the model plant *Arabidopsis thaliana* and the crop plant maize (*Zea mays*). We identified sequence features contributing to terminator strength and quantified their effect on transcript levels. By measuring terminator strength in two assay systems—tobacco leaves and maize protoplasts—we detected similarities and differences in the terminator grammar of monocotyledonous and dicotyledonous plants. Leveraging our large dataset, we trained computational models that accurately predict terminator strength. We used these models to design robust synthetic plant terminators for future crop engineering efforts.

RESULTS

Measuring the strength of plant terminators with Plant STARR-seq

To assess the strength of plant terminators at high throughput, we used Plant STARR-seq, a massively parallel reporter assay that measures the activity of *cis*-regulatory elements (Tobias Jores et al. 2020, 2021). We define a terminator as the 170 nucleotide sequence from position -150 to +20 relative to a cleavage and polyadenylation site (position 0). We used experimentally derived primary cleavage sites to select terminator sequences from *Arabidopsis* and maize (Jafar et al. 2019; Thomas et al. 2012; Wu et al. 2011). For the 3,754 *Arabidopsis*

genes that were not represented in these datasets, we used the end of the 3' untranslated region (UTR) annotation in TAIR10 as the cleavage site. Since alternative polyadenylation plays an important role in gene regulation by creating different mRNA isoforms (Arthur G. Hunt 2011), we sought to investigate the strength of both primary and secondary polyadenylation sites. Therefore, we included experimentally-derived, secondary cleavage sites supported by at least 30% of the total reads of a gene (Jafar et al. 2019; Thomas et al. 2012; Wu et al. 2011). As expected, the 24,529 *Arabidopsis* terminators and the 30,092 maize terminators displayed the distinctive nucleotide composition preferences of terminator sequences (Bernardes and Menossi 2020) and predominantly resided in the annotated 3' UTR region (Supplementary Fig. 1a-d).

The library of plant terminators was array-synthesized and cloned downstream of the coding sequence of a barcoded green fluorescent protein (GFP) reporter gene driven by the cauliflower mosaic virus 35S promoter (Fig. 1a). The plasmid library was transiently expressed in tobacco leaves or maize protoplasts. After 1 – 2 days of incubation, the reporter mRNA was extracted, and next-generation sequencing was used to count the reporter barcodes in the input DNA and the extracted RNA. We define terminator strength as the enrichment of barcodes in RNA over DNA normalized to the enrichment of a control construct containing the 35S terminator. Thus, terminator strength in our assay reflects both transcriptional activity and RNA stability, and tends to have low values due to the normalization to the highly active 35S terminator.

We performed two biological replicates in tobacco leaves and maize protoplasts. The results were highly correlated in both assay systems (Fig. 1b, c). Similarly, retesting of over 400 terminators in a second, independent library showed that the replicates in this validation experiment were highly correlated with each other and with the results of the first, large-scale experiment (Supplementary Fig. 2). Therefore, we used the average terminator strength from both replicates of the large-scale experiment for all further analyses. Terminator strength spanned a wide range of activity, allowing us to disentangle the signals that contribute to this strength. In tobacco leaves, we observed more than 64-fold difference between strong and weak terminators. Similar to previous studies (Tobias Jores et al. 2021, 2020), the dynamic range was lower in maize protoplasts, in which we detected a 16-fold difference between strong and weak terminators.

To ensure that we measured terminator strength, we included negative controls derived from coding regions in *Arabidopsis* and maize and from randomized sequences. The random sequences were generated such that their overall (global random) or per-position (positional random) nucleotide frequencies resembled that of an average *Arabidopsis* or maize terminator (Supplementary Fig. 1e-g). In both tobacco leaves and maize protoplasts, sequences derived from plant terminators outperformed these coding sequences and random controls (Fig. 1d, e). Of all control sequences, the positional random sequences showed the greatest strength, likely because they most closely resemble actual terminators. Together, these findings demonstrate that our assay captures *bona fide* terminator strength.

Most plant transgenes use viral or bacterial terminators, such as the 35S, Ag7, NOS, and MAS terminators (Andreou et al. 2021). We included these terminators in our library in their full form (not limited to 170 nucleotides) as a reference for the activity of the plant terminators. The 35S terminator, the only viral sequence in our library, outperformed almost all plant

terminators. However, some plant terminators (8 in tobacco leaves and 20 in maize protoplasts) exceeded the activity of the 35S terminator. The bacterial Ag7, NOS, and MAS terminators were far weaker than the viral 35S terminator. In tobacco leaves, we found 2,224 plant terminators that were stronger than the MAS terminator and 9,389 plant terminators that were stronger than the NOS terminator. In maize protoplasts, we found 1,369 plant terminators that were stronger than the MAS terminator and 19,585 terminators that were stronger than the NOS terminator. The strongest plant terminators are attractive alternatives to the bacterial terminators commonly used in plant transgenes.

Terminator strength correlates not with gene expression but with gene function

Next, we asked if our data could give insights into the importance of terminator strength for gene expression. We compared terminator strength determined by Plant STARR-seq with metrics related to mRNA levels, stability and degradation. We found only weak correlation between terminator strength and gene expression (Sullivan et al. 2014), mRNA half-life (Szabo et al. 2020), or nascent transcription (Liu, Zhu, and Dong 2021) (Supplementary Fig. 3). These findings corroborate reports that upstream *cis*-regulatory elements, like enhancers, promoters, and the 5' UTR, drive large-scale gene expression changes while the 3' UTR and terminators fine-tune expression levels (Washburn et al. 2019; Zrimec et al. 2020). However, the choice of terminator can have a significant impact on the expression of transgenes (F de Felippes et al. 2020; P.-H. Wang et al. 2020).

While the correlation between terminator strength and gene expression was low, we wondered whether the function of a gene and the strength of its terminator were more correlated. To address this question, we performed gene ontology (GO) term enrichment analysis on the genes associated with the strongest 10% of terminators from *Arabidopsis* or maize. For both species, we found a significant enrichment (adjusted p value < 0.05) for genes related to metabolism and response to stimulus (Supplementary Fig. 4a-d). Terminators derived from oxidoreductase-related and stress-responsive genes in *Arabidopsis* were overrepresented in the top 10% of terminators ranked by strength in tobacco leaves and maize protoplasts. Maize terminators derived from genes involved in small molecule metabolic processes were overrepresented in the strongest 10% of terminators in both systems. However, we found many more significant GO terms associated with metabolism for the strongest maize terminators in maize protoplasts than in tobacco leaves (Supplementary Fig. 4e, f). The latter finding pointed to possible species-specific differences in terminator strength, prompting us to investigate this possibility further.

Plant terminator strength is species-specific

mRNA 3' end processing may differ between monocotyledonous and dicotyledonous plants, as suggested from studies in the 1980s. For example, the gene encoding the small subunit of ribulose 1,5-bisphosphate carboxylase (*rbcS*) from the monocot wheat is improperly polyadenylated when tested in the dicot tobacco (Keith and Chua 1986). In contrast, the mRNA of the *rbcS* gene from the dicot pea is efficiently polyadenylated in tobacco (Nagy et al. 1985). Consistent with these earlier findings, we observed a relatively weak correlation (R^2 = 0.33) between the strength of a given terminator in the dicot model tobacco leaves versus the monocot model maize protoplasts (Fig. 2a). In tobacco leaves, terminators from the dicot

Arabidopsis performed significantly better than terminators from the monocot maize. Similarly, in maize protoplasts, maize terminator sequences significantly outperformed *Arabidopsis* terminators (Fig. 2b, c). These observations are consistent with species-specific differences in plant terminator strength.

Based on these observations, we wanted to identify terminators with strong species-specific activity. Since our assay systems show different dynamic ranges, we normalized terminator strength within each assay system to a scale from 0 (weakest) to 1 (strongest). We defined a variable Ψ as the difference between the normalized terminator strength in tobacco leaves and in maize protoplasts, such that a high Ψ value denotes a terminator that was considerably stronger in tobacco leaves than in maize protoplasts. We found that *Arabidopsis* terminators show a higher average Ψ value than maize terminators (Fig. 2d). We selected the top 10% of *Arabidopsis* terminators (n = 1,923) with highest Ψ values, *i.e.* tobacco-specific strength, and the top 10% of maize terminators (n = 2,439) with the lowest Ψ values, *i.e.* maize-specific strength, for GO term enrichment analysis. *Arabidopsis* terminators with highly tobacco-specific strength tended to be derived from stimulus- and stress-responsive genes, while maize terminators with highly maize-specific strength tended to be derived from metabolic genes (Fig. 2e).

To understand how species-specific terminator strength is mediated, we used STREME (Bailey 2021) to search for RNA motifs that were enriched in the tobacco-specific *Arabidopsis* terminators (high Ψ) relative to the maize-specific maize terminators (low Ψ), and *vice versa*. The most enriched motifs in the tobacco-specific *Arabidopsis* terminators were dominated by long stretches of U nucleotides, while the most enriched motifs found in maize-specific maize terminators favored G and C nucleotides (Fig. 2f, g). These findings motivated us to further analyze the effect of nucleotide composition on terminator strength.

Nucleotide composition affects terminator strength in a position-specific manner

Dicot genomes have a lower GC content than monocot genomes (Singh, Ming, and Yu 2016). This bias also holds true for *Arabidopsis* and maize terminator sequences (Fig. 3a). Assessing the impact of GC content on terminator strength, we found that terminators with either high or low GC content were weaker than those with intermediate GC content in both tobacco leaves and maize protoplasts (Fig. 3b, c). There are, however, subtle differences between the two assay systems. In tobacco leaves, terminators with a GC content around 30-35% were the strongest, while in maize protoplasts, terminators with a GC content of approximately 35-40% were the strongest. To substantiate these subtle differences, we measured the terminator strength of random sequences with a GC content of 30%, 40%, 50%, 60%, or 70%. In tobacco leaves, the random sequences with a GC content of 30% performed best, while in maize protoplasts, the random sequences with a GC content of 40% showed the highest strength (Supplementary Fig. 5). These values coincide with the average GC content of *Arabidopsis* terminators (32.5%; the average GC content of tobacco terminators is likely in a similar range) and maize terminators (40.9%). Thus, we conclude that the cleavage and polyadenylation machinery is likely attuned to the species-specific GC content of plant terminators.

Since terminator strength is governed at the RNA level, G and C or A and U nucleotides are not necessarily represented equally. Therefore, we teased apart the positional effect on

terminator strength for each of the four nucleotides (Fig. 3d, e). We found that C nucleotides have little to no effect on terminator strength in tobacco leaves or maize protoplasts. High G content was beneficial at the 5' end of our tested sequences but not tolerated near the cleavage site, especially in tobacco leaves. Conversely, high U content near the 5' end was associated with lower terminator strength. The system preferences diverged, however, for sequences with high U content starting from 100 nucleotides upstream from the cleavage site: U-rich sequences in this region were associated with increased terminator strength in tobacco leaves but not in maize protoplasts. High A content around 20 nucleotides upstream of the cleavage site was correlated with terminator strength in both systems, probably due to the canonical polyadenylation signal — a short sequence often represented by the hexamer AAUAAA — typically found at this location.

Canonical cleavage and polyadenylation motifs contribute to terminator strength

Since the strength of a terminator is only partially explained by its nucleotide composition, we searched for sequence motifs that contribute to terminator strength. To this end, we conducted a motif enrichment analysis on the strongest 25% of terminators in both assay systems. The most significantly enriched motifs match canonical cleavage and polyadenylation signals: the UGUA sequence motif from the Far Upstream Element (FUE) and the AAUAAA polyadenylation signal (Fig. 4a). While these motifs are known to affect cleavage and polyadenylation, our assay allowed us to determine the quantitative contribution of each motif to terminator strength.

The UGUA motif is highly prevalent in our library, with 60% to 80% (small differences between the UGUA-containing motifs identified by STREME lead to different numbers of positive terminators) of all terminators containing this motif. The UGUA motif is predominantly located 30 to 40 nucleotides upstream of the cleavage site in both *Arabidopsis* and maize terminators (Supplementary Fig. 6a, b). In tobacco leaves and maize protoplasts respectively, terminators with a UGUA motif were on average 50% and 20% stronger than those without this motif (Fig. 4b, c).

The polyadenylation signal is less prevalent in our library (15% to 35% of all terminators) but shows a distinct localization profile, with a sharp peak about 20 nucleotides upstream of the cleavage site (Supplementary Fig. 6c, d). The polyadenylation signal contributes significantly to terminator strength. In tobacco leaves and maize protoplasts respectively, terminators with a polyadenylation motif were 40% and 20% stronger than those without this motif (Fig. 4b, c). Since fewer than half of the terminators in our library contain a canonical polyadenylation signal, we asked if similar sequences are functionally equivalent. Terminators with a perfect AAUAAA sequence were stronger than terminators with a sequence that differs by a single nucleotide (carrying a single-nucleotide variant of this motif), although AAUAAG and AAUAAU motifs performed nearly as well. Terminators without any AAUAAA-like sequence were considerably weaker (Supplementary Fig. 7a, b).

In addition to the AAUAAA and UGUA motifs (A. G. Hunt 1994; Felipe F. de Felippes and Waterhouse 2023), we found novel U- and G-rich motifs enriched in the strongest terminators (Fig. 4a). These U/G-rich motifs are broadly distributed upstream of the polyadenylation signal and at slightly higher frequency just upstream or downstream of the cleavage site (Supplementary Fig. 6e, f). While the U/G-rich motifs share a similar localization

pattern, there are striking differences between the motifs discovered in the tobacco leaf and the maize protoplast system. The motif detected in the tobacco leaf data is found in nearly 90% of all terminators and consists of a G nucleotide surrounded by 2 to 3 U nucleotides. In contrast, the motif identified in the maize protoplast data is much less prevalent (16% of all terminators) and consists of alternating U and G nucleotides (Fig. 4a). Despite these differences, both motifs have an influence on terminator strength, leading to a 40% and 20% increase in strength for terminators with the motif as compared to those without, in tobacco and maize respectively (Fig. 4b, c).

While each individual motif contributes positively to terminator strength, we observed additive effects when multiple motifs are present within the same terminator. Independent of the assay system, the strongest terminators contain all three motifs and were on average 60% more active than terminators without any motifs (Fig. 4d, e).

To validate the effect of the identified AAUAAA and UGUA motifs on terminator strength, we selected 20 terminators each with a single strong AAUAAA or UGUA motif and generated single or double nucleotide mutations to break the motif. The terminator strength of the original and mutated sequences was then measured in tobacco leaves and maize protoplasts. Most motif mutations lowered terminator strength (Supplementary Fig. 7c, d). Mutations in the AAUAAA motif caused, on average, a 24% decrease in terminator strength in tobacco leaves and a 16% decrease in maize protoplasts. Mutations in the UGUA motif decreased terminator strength by approximately 13% and 7% in tobacco leaves and maize protoplasts, respectively.

Next, we wondered if we could use the enriched motifs to improve the strength of weak terminators. We selected randomized sequences from our initial data that showed low terminator strength and did not contain an AAUAAA, a UGUA, or a U/G-rich motif. We then inserted a CA dinucleotide at the predicted cleavage site (position 150) and added all possible single, double, and triple combinations of the AAUAAA, UGUA, and U/G-rich motifs. All sequences were then subjected to Plant STARR-seq in tobacco leaves and maize protoplasts. In most cases, adding motifs increased terminator strength and additive effects were observed when multiple motifs were inserted into a terminator (Fig. 4f, g). On average, single motifs led to a 5% to 20% increase in terminator strength. Terminators with all three motifs were approximately 60% stronger than motif-less terminators in tobacco leaves and maize protoplasts. Although the GUGUG motif was originally identified in data from the maize protoplast system, it also increased terminator activity in tobacco leaves. Taken together, these findings demonstrate that the motifs enriched in strong terminators are indeed contributing to terminator strength.

Computational models accurately predict terminator strength

Computational models can successfully predict the activity of regulatory elements by learning key sequence features (Cuperus et al. 2017; Griesemer et al. 2021; Tobias Jores et al. 2021). To develop computational models that can predict terminator strength, we initially focused on using k-mer counts as a proxy for terminator activity. To test the validity of this approach, we counted the occurrence of all possible 6-mers (4,096 sequences) in the terminator sequences, and calculated the correlation between terminator strength and how often a given 6-mer was represented in a terminator sequence. As expected, we found that the 6-mers most correlated with terminator strength in tobacco leaves and maize protoplasts are variations of the

canonical cleavage and polyadenylation signals AAUAAA and UGUA (Fig. 5a, b). However, we observed only a moderate conservation of the 6-mer rank orders between the two assay systems (Spearman's ρ = 0.29; Fig. 5c). 6-mers that were highly correlated with terminator strength in tobacco leaves but not in maize protoplasts were U-rich. Conversely, 6-mers with a high correlation to terminator strength in maize protoplasts but not in tobacco leaves were rich in G and C nucleotides (Fig. 5c, d). These findings are consistent with our prior observations on sequence motifs associated with high terminator activity, both within and across the two assay systems. Therefore, we used 6-mer counts as input features to train a lasso regression model to predict terminator strength. The model was trained on 70% of our terminator data and tested on 30% of the data. The lasso regression model had moderate predictive power, explaining 28% of the variance in terminator strength in tobacco leaves and 41% in maize protoplasts (Fig. 5e, f).

To build a model with increased predictive power, we turned to a convolutional neural network with a DenseNet architecture (Huang et al. 2017), because this approach had worked well with Plant STARR-seq data previously (Deng et al. 2023). Our DenseNet model uses the sequence of a terminator as an input and predicts the strength of this sequence in tobacco leaves and maize protoplasts. After the model was trained on 90% of the terminator data, it could accurately predict terminator strength for the remaining 10% of the data. The features learned by the model explained 76% and 67% of the variance in terminator strength in tobacco leaves and maize protoplasts, respectively (Fig. 6a, b). To understand what features the DenseNet model had learned, we used DeepLIFT and TF-MoDISco to extract consolidated sequence motifs that positively or negatively impact terminator strength (Shrikumar, Greenside, and Kundaje 2017; Shrikumar et al. 2018) prediction (Fig. 6c-f). According to this analysis, AAUAAA and UGUA motifs are associated with increased terminator strength in both assay systems. U-rich sequences decrease terminator strength in maize protoplasts, especially if they surround a UGUA motif. In contrast, U-rich sequences increase terminator strength in tobacco leaves, although this effect can be reversed by GG dinucleotides (Fig. 6e, f). These findings are consistent with the results from our motif enrichment and k-mer analyses and indicate that the DenseNet model has learned biologically relevant terminator features.

In silico evolution of terminator sequences

While our previous attempts to improve terminator strength by adding polyadenylation and cleavage motifs were successful, the gain in terminator strength was modest (Fig. 4f, g). *In silico* evolution using convolutional neural network models can drastically improve the activity of regulatory elements (Cuperus et al. 2017; Tobias Jores et al. 2021). Therefore, we used our DenseNet model for *in silico* evolution of 222 terminators,111 each from *Arabidopsis* and maize. As starting sequences, we randomly selected terminators from the held-out test set used to validate the DenseNet model. For each terminator, we generated every possible single-nucleotide substitution variant and scored these variants with the DenseNet model. We kept the variant with the highest predicted terminator strength and subjected it to another round of evolution for a maximum of ten rounds (Fig. 7a). We performed this process three times using the prediction for either tobacco leaves or maize protoplasts, or the sum of both predictions to identify the strongest variant. To test the evolved elements experimentally, we synthesized the starting sequences and those obtained after three and ten rounds of evolution, and assayed their terminator strength in tobacco leaves and maize protoplasts.

After three rounds of evolution (*i.e.*, after changing only three nucleotides), terminator strength increased, on average, 5-fold in tobacco leaves and 1.6-fold in maize protoplasts (Fig. 7b, c). For sequences obtained after ten rounds of evolution, a further increase in terminator strength was observed. Even though the original sequences and those obtained after *in silico* evolution differed by only ten nucleotides, the difference in their terminator strength was 12-fold in tobacco leaves and 4-fold in maize protoplasts (Fig. 7b, c). As expected, the increase in terminator strength was most pronounced when the prediction used to score variants during *in silico* evolution matched the experimental assay system (*i.e.* using the tobacco leaf prediction for evolution, and testing the resulting terminators in tobacco leaves). Although all starting sequences were weaker than the 35S terminator, our *in silico* evolution approach generated several terminators of greater strength than this highly active viral terminator (Fig. 7b, c).

Cleavage and polyadenylation efficiency affects terminator strength

Over 70% of the genes in *Arabidopsis* and maize contain more than one possible polyadenylation site and can therefore give rise to transcript isoforms that differ in 3' UTR length (Jafar et al. 2019; Wu et al. 2011). Alternative polyadenylation can have a strong effect on transcript levels through the inclusion or exclusion of regulatory features such as binding sites for microRNAs or RNA-binding proteins (Bernardes and Menossi 2020). We wondered whether the terminator strength of putative polyadenylation sites affects the choice of which site is used. To address this question, we measured the terminator strength of primary and secondary cleavage and polyadenylation sites from over 5000 genes. However, there was no difference between the terminator strength of primary and secondary polyadenylation sites for *Arabidopsis* or maize terminators (Supplementary Fig. 8).

While terminator strength could not predict which potential polyadenylation site is more likely to be used in a genomic context, we wondered if the reverse were true: Is the strength of a terminator associated with the efficiency of its cleavage and polyadenylation? To determine the cleavage and polyadenylation sites in our terminators, we subjected the output RNA from a Plant STARR-seq experiment in tobacco leaves to 3' end sequencing (Fig. 8a). We defined the cleavage and polyadenylation sites for each terminator as local maxima in the distribution of the cleavage positions along the terminator sequence for all unique reads. As expected, the vast majority of the cleavage and polyadenylation sites identified by this approach coincided with a CA or UA dinucleotide (Fig. 8b).

The terminators in our library were designed to contain a cleavage site at position 150 (Fig. 1a). About 61% of the terminators showed a cleavage site within 5 nucleotides upstream or downstream of this position, and for approximately half of these (32% of all terminators), this was the primary cleavage site (Table 1). Of the 54,825 terminators for which we could call cleavage sites, 68% had more than one cleavage sites, and of those, 20% (about 13% of all terminators) had a prominent secondary cleavage site indicated by at least 30% of the reads (Table 1; see Fig. 8c for examples). However, 17% of the tested sequences were not cleaved and polyadenylated but showed read-through into the downstream T-DNA sequence.

We observed differences in the cleavage pattern between *bona fide* terminators and control sequences (Fig. 8d and Table 1). Plant terminators were predominantly cleaved at position 150. In contrast, randomized sequences showed a broad distribution of cleavage sites throughout their sequence. However, for the positional random sequences which resemble

terminators more closely than the global random controls, the distribution was shifted towards an enrichment of cleavage at or near position 150. Finally, control sequences derived from coding regions were rarely cleaved and polyadenylated, consistent with a selection against potential cleavage sites. These general trends held true when considering all cleavage sites, in addition to primary sites (Supplementary Fig. 9).

Next, we tested the association of terminator strength and cleavage probability (*i.e.*, the likelihood of a terminator being cleaved and polyadenylated instead of allowing read-through transcription). Cleavage probability was strongly correlated with terminator strength (Fig. 8e, f), and terminators with a primary cleavage site within their sequence were approximately 40% stronger than those without (Fig. 8g). Furthermore, terminators with a dominant cleavage site (*i.e.*, most transcripts are cleaved at this site) were stronger terminators than those with multiple weak cleavage sites (Fig. 8f). Taken together, the efficiency and accuracy with which a terminator is cleaved and polyadenylated determines its strength. Strong terminators show a dominant cleavage site and prevent read-through into downstream sequences.

Polyadenylation motifs and GC content control cleavage probability

Since cleavage probability and terminator strength were positively correlated, we asked if the same features that influence terminator strength also affect cleavage probability. First, we tested if biological terminator function was associated with a high cleavage probability. Indeed, plant terminators showed a much higher cleavage probability than control sequences from coding regions (Fig. 9a). Randomized control sequences with a nucleotide composition similar to an average terminator were also significantly more likely to be cleaved and polyadenylated than the coding region controls, but their average cleavage probability was still lower than that of *bona fide* plant terminators. The cleavage probability for sequences derived from *Arabidopsis* was higher than the one for maize sequences (Fig. 9a).

As GC content is one of the key differences between terminators from *Arabidopsis* and maize, we asked if cleavage probability was affected by GC content. We observed a strong negative correlation (Pearson's $r = -0.65$) between these two factors. While a high AT content was associated with a high cleavage probability, increasing GC content led to decreased cleavage probability (Fig. 9b). This finding likely explains why maize sequences, which show on average an approximately 10% higher GC content than *Arabidopsis* sequences, were less likely to be cleaved than *Arabidopsis* sequences. Although both terminator strength and cleavage probability were affected by GC content, they followed different trends. Cleavage probability decreased monotonically with increasing GC content, while terminator strength was highest at an intermediate GC content and lowest in very AT- or GC-rich sequences (Fig. 3b, c). Similarly, we observed differing and position-specific effects of local nucleotide composition on terminator strength, whereas for cleavage probability, positional effects were much less pronounced, and A and T nucleotides behaved mostly similar to each other as did G and C nucleotides (Fig. 9c).

Finally, we tested if the AAUAAA, UGUA and U/G-rich motifs affected cleavage probability. While all three motifs increased cleavage probability, the AAUAAA motif clearly had the largest effect (Fig. 9d). As for terminator strength, we observed additive effects of the motifs on cleavage probability, and terminators with all three motifs were most likely to be cleaved and polyadenylated.

DISCUSSION

Here, we adapted Plant STARR-seq to characterize and optimize plant terminator sequences. We find that thousands of *Arabidopsis* and maize terminators outperformed the commonly used bacterial NOS and MAS terminators; a handful even outperformed the viral 35S terminator. These results provide a large arsenal of diverse and strong plant terminators to use with transgenes, which should alleviate transgene silencing (Diamos and Mason 2018) . The optimal terminators to employ in constructing transgenes may be those with high cleavage probability, as these prevent the read-through transcription implicated in silencing (F de Felippes et al. 2020). Thus, for use in dicots, good terminators to choose would be those from the *Arabidopsis* genes AT3G46230 (HEAT SHOCK PROTEIN 17.4), AT2G05530, and AT4G39730 (PLAT DOMAIN PROTEIN 1); for use in monocots, good ones would be those from the maize genes Zm00001d016542 (anthranilate 1,2-dioxygenase), Zm00001d047961, and Zm00001d017119 (glucose-6-phosphate dehydrogenase 5).

In addition to these naturally occurring terminators, *in silico* evolved, synthetic terminator sequences — several of which showed greater strength than the viral 35S terminator — resulted from this work. Use of the DenseNet prediction that best matched the assay system (the tobacco leaf prediction for dicots, and the maize protoplast prediction for monocots) led to the best results; however, a combination of both predictions can generate terminators that are active across a broad range of plant species, tissues, and applications. The iterative *in silico* evolution and testing of evolved elements in Plant STARR-seq appears to be a promising generalizable path toward improving the features of plant regulatory elements, as for core promoters (Tobias Jores et al. 2021; T. Jores et al. 2023).

Beyond the practical benefits of this study, we identified novel features of terminator biology in plants. We found that GC content profoundly influences terminator strength and cleavage probability in different ways. The strongest terminators had a GC content of approximately 30 – 40% (depending on the assay system), with terminator strength lowest at either higher or lower GC percentage in both assay systems. In contrast, cleavage probability monotonically decreased with increasing GC content in tobacco leaves (and was not measured in maize protoplasts due to technical challenges). This negative correlation is similar to the effects of GC content on core promoter strength, which shows a strong negative correlation with GC content in tobacco leaves but not in maize protoplasts (Tobias Jores et al. 2021). Taken together, GC content appears to affect different regulatory elements in different ways, and these effects vary across species, reflecting genomic GC content.

In addition to known polyadenylation motifs (A. G. Hunt 1994; Bernardes and Menossi 2020; Felipe F. de Felippes and Waterhouse 2023), we discovered novel motifs that increased terminator strength and cleavage probability. These motifs are rich in U and G nucleotides and reside broadly across terminator sequences, with a moderate enrichment immediately upstream and downstream of the cleavage site. The precise composition of these U/G-rich motifs differed between the tobacco leaf and the maize protoplast systems; however, the maize-specific motif also contributed to terminator strength in tobacco leaves. Human terminators contain a GU-rich element downstream of the cleavage site that is required for efficient polyadenylation and that is bound by the cleavage-stimulating factor (CSTF) complex (Beyer, Dandekar, and Keller 1997; Takagaki and Manley 1997; B. Tian and Graber 2012). Plant homologs for members of the CSTF complex can form a similar complex and bind to RNA (Arthur G. Hunt, Xing, and Li 2012;

Yao et al. 2002; Bell and Hunt 2010). We speculate that the novel U/G-rich motifs identified here serve as binding sites for the plant CSTF complex.

The assay design employed here provided insight into cleavage probability and alternative polyadenylation. Alternative polyadenylation is a crucial mechanism to create diverse transcripts in response to environmental change and in particular tissues (Bernardes and Menossi 2020; Wu et al. 2011; Ye et al. 2019). Alternative polyadenylation produces transcripts with altered 3' UTR length, resulting in different mRNAs and translation levels. Long 3' UTRs decrease transcript stability by triggering nonsense-mediated mRNA decay (Kertesz et al. 2006), while short 3' UTRs make translation more efficient by promoting polysome formation (Chang et al. 2015). When we compared the 170 nucleotide-terminator sequences of *Arabidopsis* and maize genes derived from primary vs. secondary polyadenylation sites, we observed no difference in terminator strength among sites derived from *Arabidopsis* or maize. These comparisons suggest that the sequence surrounding a given polyadenylation site does not fully explain alternative polyadenylation. T*rans*-acting factors such as the components of the cleavage and polyadenylation complexes, RNA-binding proteins and non-coding RNAs are involved in the choice of polyadenylation sites, presumably by recognizing sequence context and secondary structure of the entire terminator sequence instead of the shorter terminator sequences tested here (Zhang et al. 2020; Arthur G. Hunt 2022; Bernardes and Menossi 2020). A comparison of all tested terminator sequences indicates that strong terminators tended to contain a dominant cleavage site rather than multiple weaker ones.

METHODS

Library Design and Construction

For this study, we defined terminators as the sequence from 150 nucleotides upstream to 20 nucleotides downstream of a cleavage and polyadenylation site. For *Arababidopsis*, we used experimentally determined cleavage and polyadenylation sites described by Thomas *et al. (Thomas et al. 2012)*. We selected the primary cleavage and polyadenylation sites for each gene (n = 18,450), as well as prominent secondary cleavage sites that had at least 30% of total reads per gene (n = 2,325). For the 3,754 genes without an experimentally defined cleavage site, we utilized the end of their 3' UTR annotation in the *Arabidopsis* TAIR10 annotation as the cleavage site. This yielded a total of 24,529 *Arabidopsis* terminator sequences (Supplementary Table 1). For maize, we used cleavage and polyadenylation sites defined by Jafar *et al. (Jafar et al. 2019)*. We selected primary cleavage sites for 25,685 maize genes, and included 4,407 secondary cleavage sites (at least 30% of total reads per gene) for a total of 30,092 maize terminator sequences (Supplementary Table 1).

In addition to *bona fide* terminators, several control sequences were added to the library (Supplementary Table 1). Since protein coding sequences should not contain cleavage and polyadenylation motifs, 170-nucleotide long sequences (589 each from *Arabidopsis* and maize) from coding regions with a similar GC content as the terminator library were included as negative controls. Furthermore, we generated random sequences with global (200 sequences per species) or position-specific (1,000 sequences per species) nucleotide frequencies derived from the average *Arabidopsis* or maize terminator. Randomized sequences with a GC content of 30%, 40%, 50%, 60%, or 70% (200 sequences of 170 nucleotides each) were added to test effects of GC content on terminator strength. Finally, four commonly used non-plant terminators

(t35S, tAg7, tNOS, and tMAS) were added as a frame of reference in their full length (35S=204 nt, Ag7=208 nt, MAS= 253 nt, NOS=253 nt). The final library of sequences was ordered as an oligo pool from Twist Biosciences (Supplementary Table 2).

To validate and extend our findings from the large-scale terminator library, we created a second, smaller library. This library included 187 terminators from the original library to test the correlation between results from the two libraries. Additionally, we added sequences to validate the importance of the discovered motifs. We picked 20 sequences from the randomized control sequences in our original library that had neither a CA dinucleotide at the predicted cleavage site, nor an AAUAAA, a UGUA, or a GUGUG motif. For each validation sequence, we added a CA dinucleotide at position 150 and all possible combinations of these three motifs at the positions where they are found most often in our library. To test the importance of the AAUAAA motif, we picked twenty terminators that had only one AAUAAA sequence and generated three variants with a mutation in this sequence (ACTCAA, ACTCAA, ACTAAA). Similarly, we took twenty sequences that had only one UGUA sequence and replaced it with mutated variants (UGCA, CGUA, UCUA). Finally, we included the sequences from the *in silico* evolution (see below) in this validation library (Supplementary Table 3).

The Plant STARR-seq plasmid pPSt (https://www.addgene.org/203590/) used in this study is based on the pPSup plasmid (https://www.addgene.org/149416/) (Tobias Jores et al. 2020) with adaptations to enable the characterization of terminators. The base plasmid pPSt contains three consecutive Golden Gate cloning sites. To generate the terminator libraries, we first inserted the 35S promoter together with a 5' UTR derived from the maize histone H3 gene Zm00001d041672, an ATG start codon, and a 18-nucleotide random barcode (VNNVNNVNNVNNVNN; V = A, C or G) into the upstream Golden Gate site using the restriction enzyme BbsI-HF (NEB). Next, we cloned the array-synthesized terminator library into the downstream Golden Gate site using the restriction enzyme Esp3I (NEB). In this step, the plasmid library was bottlenecked to approximately 1,000,000 variants (approximately 16 barcodes per terminator) or 60,000 variants (approximately 30 barcodes per terminator) for the large-scale or the validation library, respectively. Finally, we used BsaI-HFv2 (NEB) to replace the central Golden Gate site with the coding sequence of GFP lacking the start codon. Two versions of the library were created in this step: one with full-length GFP for use in Plant STARR-seq (see https://www.addgene.org/203592/ for an example of a fully assembled Plant STARR-seq plasmid with the 35S terminator.) and one with a truncated version of GFP lacking the central 188 amino acids for subassembly (see below). The sequences of all primers used for cloning and sequencing are included in Supplementary Table 4.

Tobacco cultivation and transformation

Tobacco (*Nicotiana benthamiana*) was grown in soil (Sunshine Mix no. 4) at 25°C with a long day photoperiod (16 h light and 8 h dark; cool-white fluorescent lights Philips TL-D 58 W/840; intensity 300 µmol m^{-2} s^{-1}). Plants were transformed approximately 3 weeks after germination. The *Agrobacterium* transformation and induction method was previously described (Tobias Jores et al. 2021). The terminator libraries were introduced into *Agrobacterium tumefaciens* strain GV3101 (harboring the virulence plasmid pMP90 and the helper plasmid pMisoG) by electroporation. *Agrobacterium* cultures were infiltrated into the first two mature leaves of tobacco plants (12 plants/24 leaves per replicate for the large-scale library; 3 plants/6

leaves for the smaller validation library). The plants were further grown for 48 hours under normal light conditions before mRNA extraction. The input sample for Plant STARR-seq was obtained from 20 mL of the *Agrobacterium* solution that was used to infiltrate tobacco leaves. To this end, the QIAprep Spin Miniprep Kit was used according to the manufacturer's instructions.

Maize mesophyll protoplast generation and PEG transformation

We used the PEG transformation method of maize mesophyll protoplasts as described in (Tonnies et al. 2023). Maize (*Zea mays* L. cultivar B73) seeds were soaked in water overnight at 25°C. The seeds were germinated in soil for 3 days under long day conditions (16 hours light, 8 hours dark) at 25°C, then moved to complete darkness at 25°C for 10-11 days. From each seedling, 10 cm sections from the second and third leaf were cut into thin 0.5 mm strips perpendicular to veins and immediately submerged in 10 ml of protoplasting enzyme solution (0.6 M mannitol, 10 mM MES ph 5.7, 15 mg/ml cellulase R10, 3 mg/ml macerozyme, 1 mM $CaCl_2$, 0.1% [w/v] BSA, and 5 mM beta-mercaptoethanol). The mixture was covered in foil to keep out light, vacuum infiltrated for 3 min at room temperature (RT), and incubated on a shaker at 40 rpm for 2.5 hours at RT. Protoplasts were released by incubating an extra 10 min at 80 rpm. To quench the reaction, 10 mL ice-cold MMG (0.6 M Mannitol, 4 mM MES ph 5.7, 15 mM $MgCl_2$) was added to the enzyme solution and the whole solution was filtered through a 40 µM cell strainer. To pellet protoplasts, the filtrate was split into equal volumes of no more than 10 mL in chilled round-bottom glass centrifuge vials and centrifuged at 100 x g for 4 min at RT. Pellets were resuspended in 1 mL cold MMG each and combined into a single round-bottom vial. To wash, MMG was added to make a total volume of 5 mL and the solution was centrifuged at 100 x g for 3 min at RT. This wash step was repeated two more times. The final pellet was resuspended in 1-2 mL of MMG. A sample of the resuspended protoplasts was diluted 1:20 in MMG and used to count the number of viable cells using Fluorescein Diacetate as a dye.

For each replicate, 20 million protoplasts were mixed with 200 µg of the terminator plasmid library in a fresh tube, topped with MMG to a volume of 2,288 µL, and incubated on ice for 30 min. For PEG transformation, 2,112 µL of PEG solution (0.6 M Mannitol, 0.1 M $CaCl_2$, 25% [w/v] poly-ethylene glycol MW 4000) was added to reach a final concentration of 12% (w/v) PEG. The mixture was incubated for 10 min in the dark at RT. After incubation, the transformation solution was diluted with 22 mL (5 x 4.4 mL) incubation solution (0.6 M Mannitol, 4 mM MES pH 5.7, 4 mM KCl), and centrifuged at 100 x g for 4 min at RT. For the PEG transformation with the validation library, we used 4 million protoplasts, 40 µg of the plasmid library, and one fifth of the buffer volumes used for the large-scale library.

After transformation, the protoplast pellet was washed with 5 mL of incubation solution, centrifuged at 100 x g for 3 min at RT, and resuspended in incubation solution to a concentration of 500 cells/µL. Protoplasts were incubated overnight in the dark at RT to allow for transcription of the plasmid library and then pelleted (4 min, 100 x g, RT). The pellet was washed with 5 mL incubation solution and centrifuged (3 min, 100 x g, RT). The pellet was finally resuspended in 5 mL incubation solution. An aliquot of the solution was used to check transformation efficiency under a microscope (12.4% [replicate 1] and 49.5% [replicate 2] transformation efficiency for the large-scale library; 62% [replicate 1] and 45% [replicate 2] for the validation library). Cells were pelleted (4 min, 100 x g, RT) and resuspended in 2 mL Trizol

for subsequent mRNA extraction. An aliquot of the plasmid library used for PEG transformation was used as the input sample for Plant STARR-seq.

Plant STARR-seq assay

For all Plant STARR-seq experiments, two independent biological replicates were performed. Different plants and fresh *Agrobacterium* cultures were used for each biological replicate.

Tobacco leaves were harvested 2 days after infiltration and partitioned into batches of 4 (large-scale library) or 3 (validation library) leaves. The leaf batches were frozen in liquid nitrogen, finely ground with mortar and pestle, and immediately resuspended in 12 mL Trizol. The suspensions were cleared by centrifugation (5 min, 4,000 x g, 4°C) and each supernatant was mixed with 2.5 mL chloroform. After centrifugation (15 min, 4,000 x g, 4°C), 7 mL of the upper, aqueous phase was transferred to a new tube, and mixed by inversion with 3.5 mL high salt buffer (0.8 M sodium citrate, 1.2 M NaCl) and 3.5 mL isopropanol. The solution was incubated for 15 min at RT to precipitate the RNA and centrifuged (30 min, 4,000 x g, 4°C). The pellet was washed in 10 mL ice-cold 70% ethanol, centrifuged (5 min, 4000 x g, 4°C), and air-dried. The pellet was resuspended in 180 µL of warm (65°C) nuclease-free water and transferred to a new tube. The solution was supplemented with 10 µL 20X DNase I buffer (1 mM $CaCl_2$, 100 mM Tris pH 7.4), 10 µL 200 mM $MnCl_2$, 2µL DNase I (ThermoFisher Scientific), and 1 µL RNaseOUT (ThermoFisher Scientific), and incubated for 30 min at 37°C. To precipitate the RNA, 20 µL 8M ice-cold LiCl and 500 µL ice-cold 100% ethanol was added. After incubation for 15 min at -80°C, the RNA was pelleted by centrifugation (20 min, 20,000 x g, 4°C). The pellet was washed with 500 µL ice-cold 70% ethanol, centrifuged (5 min, 20,000 x g, 4°C), air-dried for 10 min, and resuspended in 200 µL nuclease-free water supplemented with 0.5 µL RNaseOUT. For cDNA synthesis, eight reactions with 11 µL mRNA solution, 1 µL 2 µM GFP-specific reverse transcription primer, and 1 µL 10 mM dNTPs were incubated at 65°C for 5 min then immediately placed on ice. The reactions were supplemented with 4 µL 5X SuperScript IV buffer, 1 µL 100 mM DTT, 1 µL RNaseOUT, and 1 µL SuperScript IV reverse transcriptase (ThermoFisher Scientific). To ensure that the samples were largely free of DNA contamination, four reactions were used as controls, where the reverse transcriptase and RNaseOUT were replaced with water. Reactions were incubated for 10 min at 55°C, followed by 10 min at 80°C. Sets of 4 reactions each were pooled. The cNDA was purified with the Zymo Clean&Concentrate-5 kit, and eluted in 20 µL 10 mM Tris. The barcode was amplified with 10-20 cycles of polymerase chain reaction (PCR) and read out by next generation sequencing.

For Plant STARR-seq in maize protoplasts, the protoplast-containing Trizol solution from PEG transformation was transferred to 2 mL Phasemaker tubes (1 mL per tube; ThermoFisher Scientific), mixed thoroughly with 300 µL chloroform, and centrifuged (5 min, 15,000 x g, 4°C). RNA was extracted using the RNeasy Plant Mini Kit (QIAGEN). The supernatant was transferred to a QIAshrededer column and centrifuged (2 min, 20,000 x g, RT). The flowthrough was transferred to a new 1.5 mL tube and mixed with 300 µL 100% ethanol. Up to 500 µL of the solution was loaded on an RNeasy mini spin column. After centrifugation (10 seconds, 16,100 x g, RT) the flowthrough was discarded. This was repeated until all the solution had been added to the column. The column was washed once with 700 µL RW1 buffer and twice with 500 µL RPE buffer. After each wash step, the column was centrifuged (30 sec, 16,100 x g, RT) and the

flowthrough was discarded. The column was dried with an extra centrifugation step (30 sec, 16,100 x g, RT) and transferred to a 1.5 mL collection tube. For elution, 50 µL of RNase-free water was added, and the column was incubated for 1 minute, and centrifuged (1 min, 16,100 x g, RT). This elution step was repeated with an additional 40 µL of RNase-free water. The eluate was treated with DNase I (5 µL of 20x DNaseI buffer, 5 µL 200 mM $MnCL_2$, 1 µL RNaseOUT, and 2 µL DNase I) for 1 h at 37°C. The solution was supplemented with 20 µL 500 mM EDTA, 1 µL 20 mg/mL glycogen, 12 µL ice-cold 8M LiCl, and 300 µL ice-cold 100% ethanol. The solution was incubated 15 min at -80°C, centrifuged (20 min, 20,000 x g, 4°C). The pellet was washed with 500 µL ice-cold 70% ethanol, and centrifuged (3 min, 20,000 x g, 4°C). The pellet was air-dried for 10 min and resuspended in 100 µL RNase-free water. Reverse transcription, purification, PCR amplification and sequencing were performed as for the tobacco samples.

Subassembly and barcode sequencing

Paired-end sequencing on an Illumina NextSeq 2000 platform was used to link terminators to their respective barcodes. To facilitate sequencing, we created a shortened version of the terminator library plasmid with a large deletion in the GFP gene. The terminator region was sequenced using paired 151-nucleotide reads, and two 18-nucleotide indexing reads were used to sequence the barcodes. The paired terminator and barcode reads were assembled using PANDAseq (version 2.11) (Masella et al. 2012) and the terminator reads were aligned to the designed terminator library using BowTie2 (version 2.4.1) (Langmead and Salzberg 2012). Terminator-barcode pairs with less than 5 reads and terminators with a mutation or truncation were discarded. For each Plant STARR-seq experiment, barcodes were sequenced using paired-end reads on an Illumina NextSeq 2000 system. The paired barcode reads were assembled using PANDAseq.

Computational methods

For calculating terminator strength, the reads for each barcode were counted in the input and cDNA (output) samples. Barcodes with less than five reads were discarded. For each terminator, the sum of the reads for all associated barcodes was calculated in the input and output samples. The input and output counts were normalized by dividing each by the sum of all counts in the output and input sample, respectively. Terminator strength was calculated as the normalized output counts divided by the normalized input counts. Terminator strength was normalized to the strength of the 35S terminator. We used the average terminator strength across two replicates for all analyses (Supplementary Tables 2 and 3). Spearman and Pearson's correlation were calculated using base R (version 4.3.0). Significance was calculated using the two-sided Wilcoxon rank-sum test and the ggsignif library (version 0.6.4) in R (Supplementary Table 5). GO term enrichment analysis was performed using the ggprofiler2 package (version 0.2.1) in R (Supplementary Table 6).

Discovery of terminator motifs

To find motifs enriched in strong terminators, we ranked terminators according to their strength in tobacco leaves or maize protoplasts. The sequences of the top 25% terminators were analyzed by STREME (version 5.5.1) (Bailey 2021) to find ungapped RNA motifs that are enriched in this set relative to the sequences of the bottom 25% terminators. To find tobacco-

specific terminator motifs, we used STREME with the same parameters but using the top 10% *Arabidopsis* of terminators ranked by Ψ as positive and the bottom 10% of maize terminators ranked by Ψ as negative sequences. For maize-specific terminator motifs, we repeated the analysis but switched the positive and negative sequences. Meme files with all discovered motifs are available on GitHub (https://github.com/lampoona/Terminators-Plant-STARR-seq).

All terminator sequences were analyzed using the universalmotif package (version 1.18.0) in R to find the position and frequency of the discovered motifs. For each sequence, the maximum motif score was identified and normalized to the minimum (set to 0) and maximum (set to 1) scores possible. Sequences with a score of at least 0.85 were considered to contain a motif match.

Computational modeling of terminator strength

In order to predict terminator strength, we first build a lasso regression model using the glmnet package (version 4.1.7) in R to predict terminator strength based on the counts of all possible, overlapping 6-mer counts. The regression model was trained on 70% of the data and tested on the remaining 30%.

For our second model, we built a convolutional neural net model using EUGENe (version 0.0.6) (Klie et al. 2022) and PyTorch ((Paszke et al. 2019); version 1.11.0) in Python (version 3.8.10). We used a "DenseNet" (Huang et al. 2017) architecture adapted from iCREPCP (Deng et al. 2023). The model takes one-hot encoded DNA as an input which is fed to a convolutional layer with 128 filters and a kernel size of 5. This layer is followed by four dense blocks consisting of 6, 12, 24, and 16 convolutional layers with 12 filters each and a kernel size of 3. In each dense block, the output of a convolutional layer is appended to its input and the combined output is used as the input for the subsequent layer. Between each dense block, the output feature map is reduced in size through convolution (using half as many filters as the input and a kernel size of 1) and average pooling (with a kernel size of 2). The output of the final dense block is fed into a fully connected layer with two outputs corresponding to the terminator strength in tobacco leaves and maize protoplasts, respectively. Terminator sequences from our original library that were detected in tobacco leaves and maize protoplast STARR-seq experiments (n = 53,409) were used for model training and evaluation. Of this data, 81% were used to train the model, 9% were used as a validation set during training and the remaining 10% were used to test the generalizability and accuracy of the trained model. Feature attributions for sequences in the test set were calculated using the DeepLIFT method (Shrikumar, Greenside, and Kundaje 2017) implemented in EUGENe. These feature attributions were used as input for TF-MoDISco-lite (version 2.0.6) (Shrikumar et al. 2018) to extract motifs that increase or decrease terminator strength. Since we were looking for RNA motifs, we modified the TF-MoDISco-lite algorithm to not consider reverse complemented seqlets for clustering, alignments, or pattern generation. The code for model training and evaluation, and the trained model are available on GitHub (https://github.com/lampoona/Terminators-Plant-STARR-seq).

***In silico* evolution of terminator sequences**

We used the DenseNet model to iteratively improve terminator strength. We randomly selected 222 sequences (111 each from *Arabidopsis* and maize) from the test set of our model to ensure that the model had not seen these sequences during training. In each iteration, we

generated every possible point mutation for each sequence, scored them with the DenseNet model, and kept the sequence variant with the highest predicted strength in tobacco leaves, maize protoplasts, or both (using the sum of the activity in the individual systems) systems for the next iteration. We then experimentally determined the terminator strength of the sequences after three and ten rounds of evolution using Plant STARR-seq in both tobacco leaves and maize protoplasts.

3' end sequencing

We used 3' end sequencing to determine the cleavage and polyadenylation site for each terminator. For cDNA synthesis, we incubated 5 µL of the extracted mRNA from the second Plant STARR-seq replicate in tobacco leaves with 5 µL RNase free water, 1 µL 10 mM DNTPs, and 2 µL 25 mM UMI-containing oligo-dT primer for 5 min at 55°C. The solution was supplemented with 4 µL 5X SuperScript IV buffer, 1 µL 100 mM DTT, 1 µL RNaseOUT, and 1 µL Superscript IV reverse transcriptase. The reaction was incubated for 2 min each at 4°C, 10°C, 20°C, 30°C, 40°C and 50°C, and finally for 15 min at 55°C. The sample was supplemented with 1 µL RNase H (NEB) and incubated for 30 min at 37°C. The cDNA was purified using the Zymo Clean&Concentrate-5 kit and PCR-amplified using indexed sequencing primers specific to the end of the GFP construct and the adapter added using the RT primer (Fig. 8a). Terminators were sequenced using an Illumina NextSeq 2000 platform with a 222-nucleotide read from the 5' end of the amplicon. The paired read was used to sequence the 8-nucleotide UMI. UMIs and terminator reads were linked using UMI-Tools (version 1.1.2) (Smith, Heger, and Sudbery 2017). Poly-A tails of each read were removed using CutAdapt (version 2.5) (Kechin et al. 2017). Terminators were aligned to the designed terminator library plus 52 nucleotide of plasmid backbone sequence using BowTie2 (version 2.4.1) (Langmead and Salzberg 2012) and reads that had a map quality of 0 or 1 were removed using Samtools (version 1.9) (Li et al. 2009). Duplicate terminator-UMI pairs were removed and terminators with fewer than 20 supporting reads were discarded. Bam files for each terminator were generated, and cleavage sites were determined using a custom R script available on GitHub (https://github.com/lampoona/Terminators-Plant-STARR-seq). Briefly, the algorithm identifies local maxima in the distribution of read lengths per terminator. Cleavage probability was calculated on a per terminator basis as the percentage of reads shorter than 171 nucleotides (Supplementary Table 2).

DATA AVAILABILITY

All sequencing results are deposited in the NCBI Sequence Read Archive under the BioProject accession XXX (will be made available upon publication).

CODE AVAILABILITY

The code used in this study is available on GitHub (https://github.com/lampoona/Terminators-Plant-STARR-seq).

AUTHOR CONTRIBUTIONS

All authors conceived and interpreted experiments; S.G., T.J., J.T., and N.A.M performed experiments; S.G., T.J., and K.B. analyzed the data; S.G., T.J., and T.W. did the *in silico* modeling. S.G., T.J., C.Q., and S.F prepared the manuscript and figures.

COMPETING INTERESTS

The authors declare no competing interests.

ACKNOWLEDGEMENTS

This work was supported by the National Science Foundation (RESEARCH-PGR grant no. 1748843 to E.S.B., S.F. and C.Q. and PlantSynBio grant no. 2240888 to C.Q.), the German Research Foundation (DFG; postdoctoral fellowship no. 441540116 to T.J.), the National Institute of Health (T32 training grant no. HG000035 to J.T., NIGMS grant no. R01-GM079712 to J.T.C. and C.Q., and NIGMS MIRA grant no. 1R35GM139532), and the United States Department of Agriculture (NIFA postdoctoral fellowship no. 2023-67012-39445 to N.A.M).

REFERENCES

Allen, Edwards, and Miya D. Howell. 2010. “miRNAs in the Biogenesis of Trans-Acting siRNAs in Higher Plants.” *Seminars in Cell & Developmental Biology* 21 (8): 798–804.

Andreou, Andreas I., Jessica Nirkko, Marisol Ochoa-Villarreal, and Naomi Nakayama. 2021. “Mobius Assembly for Plant Systems Highlights Promoter-Terminator Interaction in Gene Regulation.” *bioRxiv*. https://doi.org/10.1101/2021.03.31.437819.

Baeg, Kyungmin, Hiro-Oki Iwakawa, and Yukihide Tomari. 2017. “The poly(A) Tail Blocks RDR6 from Converting Self mRNAs into Substrates for Gene Silencing.” *Nature Plants* 3 (March): 17036.

Bailey, Timothy L. 2021. “STREME: Accurate and Versatile Sequence Motif Discovery.” *Bioinformatics* 37 (18): 2834–40.

Bell, Stephen A., and Arthur G. Hunt. 2010. “The Arabidopsis Ortholog of the 77 kDa Subunit of the Cleavage Stimulatory Factor (AtCstF-77) Involved in mRNA Polyadenylation Is an RNA-Binding Protein.” *FEBS Letters* 584 (8): 1449–54.

Bernardes, Willian Souza, and Marcelo Menossi. 2020. “Plant 3’ Regulatory Regions From mRNA-Encoding Genes and Their Uses to Modulate Expression.” *Frontiers in Plant Science*. https://doi.org/10.3389/fpls.2020.01252.

Beyer, K., T. Dandekar, and W. Keller. 1997. “RNA Ligands Selected by Cleavage Stimulation Factor Contain Distinct Sequence Motifs That Function as Downstream Elements in 3’-End Processing of Pre-mRNA.” *The Journal of Biological Chemistry* 272 (42): 26769–79.

Chang, Jae-Woong, Wei Zhang, Hsin-Sung Yeh, Ebbing P. de Jong, Semo Jun, Kwan-Hyun Kim, Sun S. Bae, et al. 2015. “mRNA 3′-UTR Shortening Is a Molecular Signature of mTORC1 Activation.” *Nature Communications*. https://doi.org/10.1038/ncomms8218.

Cuperus, Josh T., Benjamin Groves, Anna Kuchina, Alexander B. Rosenberg, Nebojsa Jojic, Stanley Fields, and Georg Seelig. 2017. “Deep Learning of the Regulatory Grammar of Yeast 5’ Untranslated Regions from 500,000 Random Sequences.” *Genome Research* 27 (12): 2015–24.

Dadami, Elena, Athanasios Dalakouras, Michele Zwiebel, Gabi Krczal, and Michael Wassenegger. 2014. “An Endogene-Resembling Transgene Is Resistant to DNA Methylation and Systemic Silencing.” *RNA Biology* 11 (7): 934–41.

Deng, Kaixuan, Qizhe Zhang, Yuxin Hong, Jianbing Yan, and Xuehai Hu. 2023. “iCREPCP: A Deep Learning-Based Web Server for Identifying Base-Resolution Cis-Regulatory Elements within Plant Core Promoters.” *Plant Communications* 4 (1): 100455.

Department of Economic and Social Affairs. 2022. *World Economic Situation and Prospects 2022*. United Nations.

Diamos, Andrew G., and Hugh S. Mason. 2018. “Chimeric 3’ Flanking Regions Strongly Enhance Gene Expression in Plants.” *Plant Biotechnology Journal* 16 (12): 1971–82.

Eshed, Yuval, and Zachary B. Lippman. 2019. “Revolutions in Agriculture Chart a Course for Targeted Breeding of Old and New Crops.” *Science* 366 (6466). https://doi.org/10.1126/science.aax0025.

F de Felippes, Felipe, Marcus McHale, Rachel L. Doran, Sally Roden, Andrew L. Eamens, E. Jean Finnegan, and Peter M. Waterhouse. 2020. “The Key Role of Terminators on the Expression and Post-Transcriptional Gene Silencing of Transgenes.” *The Plant Journal: For Cell and Molecular Biology* 104 (1): 96–112.

Felippes, Felipe F. de, and Peter M. Waterhouse. 2023. “Plant Terminators: The Unsung Heroes of Gene Expression.” *Journal of Experimental Botany* 74 (7): 2239–50.

Felippes, Felipe Fenselau de, Kylie Shand, and Peter M. Waterhouse. 2022. “Identification of a Transferrable Terminator Element That Inhibits Small RNA Production and Improves Transgene Expression Levels.” *Frontiers in Plant Science* 13 (May): 877793.

Griesemer, Dustin, James R. Xue, Steven K. Reilly, Jacob C. Ulirsch, Kalki Kukreja, Joe R. Davis, Masahiro Kanai, et al. 2021. “Genome-Wide Functional Screen of 3’UTR Variants Uncovers Causal Variants for Human Disease and Evolution.” *Cell* 184 (20): 5247–60.e19.

Hickey, Lee T., Amber N Hafeez, Hannah Robinson, Scott A. Jackson, Soraya C. M. Leal-Bertioli, Mark Tester, Caixia Gao, Ian D. Godwin, Ben J. Hayes, and Brande B. H. Wulff. 2019. “Breeding Crops to Feed 10 Billion.” *Nature Biotechnology* 37 (7): 744–54.

Hirai, Tadayoshi, Natsuko Kurokawa, Narendra Duhita, Kyoko Hiwasa-Tanase, Kazuhisa Kato, Ko Kato, and Hiroshi Ezura. 2011. “The HSP Terminator of Arabidopsis Thaliana Induces a High Level of Miraculin Accumulation in Transgenic Tomatoes.” *Journal of Agricultural and Food Chemistry* 59 (18): 9942–49.

Huang, Gao, Zhuang Liu, Laurens Van Der Maaten, and Kilian Q. Weinberger. 2017. “Densely Connected Convolutional Networks.” In *2017 IEEE Conference on Computer Vision and Pattern Recognition (CVPR)*. IEEE. https://doi.org/10.1109/cvpr.2017.243.

Hunt, A. G. 1994. “Messenger RNA3’end Formation in Plants.” *Annual Review of Plant Biology*. https://www.annualreviews.org/doi/pdf/10.1146/annurev.pp.45.060194.000403?casa_token=DELrTWpmoPQAAAAA:JdKLKGGrwFFsnXyfpTzZi7HGUS2T3kBVgmEiA6dOsTUevFwJKwpOr20ejVEDsXVIMOY2wc7qNFTh2Q.

Hunt, Arthur G. 2011. “RNA Regulatory Elements and Polyadenylation in Plants.” *Frontiers in Plant Science* 2: 109.

———. 2022. “Review: Mechanisms Underlying Alternative Polyadenylation in Plants - Looking in the Right Places.” *Plant Science: An International Journal of Experimental Plant Biology* 324 (November): 111430.

Hunt, Arthur G., Denghui Xing, and Qingshun Q. Li. 2012. “Plant Polyadenylation Factors: Conservation and Variety in the Polyadenylation Complex in Plants.” *BMC Genomics* 13 (November): 641.

Ingelbrecht, I. L., L. M. Herman, R. A. Dekeyser, M. C. Van Montagu, and A. G. Depicker. 1989. “Different 3’ End Regions Strongly Influence the Level of Gene Expression in Plant Cells.” *The Plant Cell* 1 (7): 671–80.

Jafar, Zehra, Salma Tariq, Irfan Sadiq, Tayyab Nawaz, and Malik Nadeem Akhtar. 2019. “Genome-Wide Profiling of Polyadenylation Events in Maize Using High-Throughput Transcriptomic Sequences.” *G3* 9 (8): 2749–60.

Jores, T., M. Hamm, J. T. Cuperus, and C. Queitsch. 2023. “Frontiers and Techniques in Plant

Gene Regulation." *Current Opinion in Plant Biology* , (in press).
Jores, Tobias, Jackson Tonnies, Michael W. Dorrity, Josh T. Cuperus, Stanley Fields, and Christine Queitsch. 2020. "Identification of Plant Enhancers and Their Constituent Elements by STARR-Seq in Tobacco Leaves." *The Plant Cell* 32 (7): 2120–31.
Jores, Tobias, Jackson Tonnies, Travis Wrightsman, Edward S. Buckler, Josh T. Cuperus, Stanley Fields, and Christine Queitsch. 2021. "Synthetic Promoter Designs Enabled by a Comprehensive Analysis of Plant Core Promoters." *Nature Plants* 7 (6): 842–55.
Kechin, Andrey, Uljana Boyarskikh, Alexander Kel, and Maxim Filipenko. 2017. "cutPrimers: A New Tool for Accurate Cutting of Primers from Reads of Targeted Next Generation Sequencing." *Journal of Computational Biology: A Journal of Computational Molecular Cell Biology* 24 (11): 1138–43.
Keith, Brian, and Nam-Hai Chua. 1986. "Monocot and Dicot Pre-mRNAs Are Processed with Different Efficiencies in Transgenic Tobacco." *The EMBO Journal*. https://doi.org/10.1002/j.1460-2075.1986.tb04516.x.
Kertesz, S., Z. Kerenyi, Z. Merai, and I. Bartos. 2006. "Both Introns and Long 3′-UTRs Operate as Cis-Acting Elements to Trigger Nonsense-Mediated Decay in Plants." *Nucleic Acids*. https://academic.oup.com/nar/article-abstract/34/21/6147/3100510.
Klie, Adam, Hayden Stites, Tobias Jores, Joe J. Solvason, Emma K. Farley, and Hannah Carter. 2022. "EUGENe: A Python Toolkit for Predictive Analyses of Regulatory Sequences." *bioRxiv*. https://doi.org/10.1101/2022.10.24.513593.
Kumar, Ananthanarayanan, Marcello Clerici, Lena M. Muckenfuss, Lori A. Passmore, and Martin Jinek. 2019. "Mechanistic Insights into mRNA 3'-End Processing." *Current Opinion in Structural Biology* 59 (December): 143–50.
Langmead, Ben, and Steven L. Salzberg. 2012. "Fast Gapped-Read Alignment with Bowtie 2." *Nature Methods* 9 (4): 357–59.
Li, Heng, Bob Handsaker, Alec Wysoker, Tim Fennell, Jue Ruan, Nils Homer, Gabor Marth, Goncalo Abecasis, Richard Durbin, and 1000 Genome Project Data Processing Subgroup. 2009. "The Sequence Alignment/Map Format and SAMtools." *Bioinformatics* 25 (16): 2078–79.
Liu, Min, Jiafu Zhu, and Zhicheng Dong. 2021. "Immediate Transcriptional Responses of Arabidopsis Leaves to Heat Shock." *Journal of Integrative Plant Biology* 63 (3): 468–83.
Loke, Johnny C., Eric A. Stahlberg, David G. Strenski, Brian J. Haas, Paul Chris Wood, and Qingshun Quinn Li. 2005. "Compilation of mRNA Polyadenylation Signals in Arabidopsis Revealed a New Signal Element and Potential Secondary Structures." *Plant Physiology* 138 (3): 1457–68.
Masella, Andre P., Andrea K. Bartram, Jakub M. Truszkowski, Daniel G. Brown, and Josh D. Neufeld. 2012. "PANDAseq: Paired-End Assembler for Illumina Sequences." *BMC Bioinformatics* 13 (February): 31.
Nagaya, Shingo, Kazue Kawamura, Atsuhiko Shinmyo, and Ko Kato. 2010. "The HSP Terminator of Arabidopsis Thaliana Increases Gene Expression in Plant Cells." *Plant & Cell Physiology* 51 (2): 328–32.
Nagy, F., G. Morelli, R. T. Fraley, S. G. Rogers, and N. H. Chua. 1985. "Photoregulated Expression of a Pea rbcS Gene in Leaves of Transgenic Plants." *The EMBO Journal* 4 (12): 3063–68.
Paszke, Adam, Sam Gross, Francisco Massa, Adam Lerer, James Bradbury, Gregory Chanan, Trevor Killeen, et al. 2019. "Pytorch: An Imperative Style, High-Performance Deep Learning Library." *Advances in Neural Information Processing Systems* 32. https://proceedings.neurips.cc/paper/2019/hash/bdbca288fee7f92f2bfa9f7012727740-Abstract.html.
Pérez-González, Ana, and Elena Caro. 2018. "Effect of Transcription Terminator Usage on the Establishment of Transgene Transcriptional Gene Silencing." *BMC Research Notes* 11 (1):

511.
Qin, Cheng, Nongnong Shi, Mei Gu, Hang Zhang, Bin Li, Jiajia Shen, Atef Mohammed, et al. 2012. “Involvement of RDR6 in Short-Range Intercellular RNA Silencing in Nicotiana Benthamiana.” *Scientific Reports* 2 (June): 467.
Rodríguez-Leal, Daniel, Zachary H. Lemmon, Jarrett Man, Madelaine E. Bartlett, and Zachary B. Lippman. 2017. “Engineering Quantitative Trait Variation for Crop Improvement by Genome Editing.” *Cell* 171 (2): 470–80.e8.
Shen, Yingjia, Guoli Ji, Brian J. Haas, Xiaohui Wu, Jianti Zheng, Greg J. Reese, and Qingshun Quinn Li. 2008. “Genome Level Analysis of Rice mRNA 3′-End Processing Signals and Alternative Polyadenylation.” *Nucleic Acids Research* 36 (9): 3150–61.
Shrikumar, Avanti, Peyton Greenside, and Anshul Kundaje. 2017. “Learning Important Features Through Propagating Activation Differences.” In *International Conference on Machine Learning*, 3145–53. PMLR.
Shrikumar, Avanti, Katherine Tian, Žiga Avsec, Anna Shcherbina, Abhimanyu Banerjee, Mahfuza Sharmin, Surag Nair, and Anshul Kundaje. 2018. “Technical Note on Transcription Factor Motif Discovery from Importance Scores (TF-MoDISco) Version 0.5.6.5.” *arXiv [cs.LG]*. arXiv. http://arxiv.org/abs/1811.00416.
Singh, Ratnesh, Ray Ming, and Qingyi Yu. 2016. “Comparative Analysis of GC Content Variations in Plant Genomes.” *Tropical Plant Biology* 9 (3): 136–49.
Smith, Tom, Andreas Heger, and Ian Sudbery. 2017. “UMI-Tools: Modeling Sequencing Errors in Unique Molecular Identifiers to Improve Quantification Accuracy.” *Genome Research* 27 (3): 491–99.
Sullivan, Alessandra M., Andrej A. Arsovski, Janne Lempe, Kerry L. Bubb, Matthew T. Weirauch, Peter J. Sabo, Richard Sandstrom, et al. 2014. “Mapping and Dynamics of Regulatory DNA and Transcription Factor Networks in A. Thaliana.” *Cell Reports* 8 (6): 2015–30.
Szabo, Emese Xochitl, Philipp Reichert, Marie-Kristin Lehniger, Marilena Ohmer, Marcella de Francisco Amorim, Udo Gowik, Christian Schmitz-Linneweber, and Sascha Laubinger. 2020. “Metabolic Labeling of RNAs Uncovers Hidden Features and Dynamics of the Arabidopsis Transcriptome.” *The Plant Cell* 32 (4): 871–87.
Takagaki, Y., and J. L. Manley. 1997. “RNA Recognition by the Human Polyadenylation Factor CstF.” *Molecular and Cellular Biology* 17 (7): 3907–14.
Thomas, Patrick E., Xiaohui Wu, Man Liu, Bobby Gaffney, Guoli Ji, Qingshun Q. Li, and Arthur G. Hunt. 2012. “Genome-Wide Control of Polyadenylation Site Choice by CPSF30 in Arabidopsis.” *The Plant Cell* 24 (11): 4376–88.
Tian, Bin, and Joel H. Graber. 2012. “Signals for Pre-mRNA Cleavage and Polyadenylation.” *Wiley Interdisciplinary Reviews. RNA* 3 (3): 385–96.
Tian, Chenfei, Yixin Zhang, Jianhua Li, and Yong Wang. 2022. “Benchmarking Intrinsic Promoters and Terminators for Plant Synthetic Biology Research.” *BioDesign Research* 2022. https://downloads.spj.sciencemag.org/bdr/2022/9834989.pdf.
Tonnies, Jackson, Mueth Nicholas Arthur, Sayeh Gorjifard, Jonah Chu, and Christine Queitsch. 2023. “Scalable Transfection of Maize Mesophyll Protoplasts.” *Journal of Visualized Experiments*, (in press).
Wang, Po-Hao, Sandeep Kumar, Jia Zeng, Robert McEwan, Terry R. Wright, and Manju Gupta. 2020. “Transcription Terminator-Mediated Enhancement in Transgene Expression in Maize: Preponderance of the AUGAAU Motif Overlapping With Poly(A) Signals.” *Frontiers in Plant Science* 11. https://doi.org/10.3389/fpls.2020.570778.
Wang, Xingang, Lyndsey Aguirre, Daniel Rodríguez-Leal, Anat Hendelman, Matthias Benoit, and Zachary B. Lippman. 2021. “Dissecting Cis-Regulatory Control of Quantitative Trait Variation in a Plant Stem Cell Circuit.” *Nature Plants* 7 (4): 419–27.
Washburn, Jacob D., Maria Katherine Mejia-Guerra, Guillaume Ramstein, Karl A. Kremling,

Ravi Valluru, Edward S. Buckler, and Hai Wang. 2019. “Evolutionarily Informed Deep Learning Methods for Predicting Relative Transcript Abundance from DNA Sequence.” *Proceedings of the National Academy of Sciences of the United States of America* 116 (12): 5542–49.

Wu, Xiaohui, Man Liu, Bruce Downie, Chun Liang, Guoli Ji, Qingshun Q. Li, and Arthur G. Hunt. 2011. “Genome-Wide Landscape of Polyadenylation in Arabidopsis Provides Evidence for Extensive Alternative Polyadenylation.” *Proceedings of the National Academy of Sciences of the United States of America* 108 (30): 12533–38.

Yao, Youli, Luhua Song, Yael Katz, and Gad Galili. 2002. “Cloning and Characterization of Arabidopsis Homologues of the Animal CstF Complex That Regulates 3’ mRNA Cleavage and Polyadenylation.” *Journal of Experimental Botany* 53 (378): 2277–78.

Ye, Congting, Qian Zhou, Xiaohui Wu, Guoli Ji, and Qingshun Quinn Li. 2019. “Genome-Wide Alternative Polyadenylation Dynamics in Response to Biotic and Abiotic Stresses in Rice.” *Ecotoxicology and Environmental Safety* 183 (November): 109485.

Zhang, Jian, Yi-Zhe Zhang, Jing Jiang, and Cheng-Guo Duan. 2020. “The Crosstalk Between Epigenetic Mechanisms and Alternative RNA Processing Regulation.” *Frontiers in Genetics* 11 (August): 998.

Zhou, Andy, Liam D. Kirkpatrick, Izaiah J. Ornelas, Lorenzo J. Washington, Niklas F. C. Hummel, Christopher W. Gee, Sophia N. Tang, Collin R. Barnum, Henrik V. Scheller, and Patrick M. Shih. 2023. “A Suite of Constitutive Promoters for Tuning Gene Expression in Plants.” *ACS Synthetic Biology* 12 (5): 1533–45.

Zrimec, Jan, Christoph S. Börlin, Filip Buric, Azam Sheikh Muhammad, Rhongzen Chen, Verena Siewers, Vilhelm Verendel, Jens Nielsen, Mats Töpel, and Aleksej Zelezniak. 2020. “Deep Learning Suggests That Gene Expression Is Encoded in All Parts of a Co-Evolving Interacting Gene Regulatory Structure.” *Nature Communications* 11 (1): 6141.

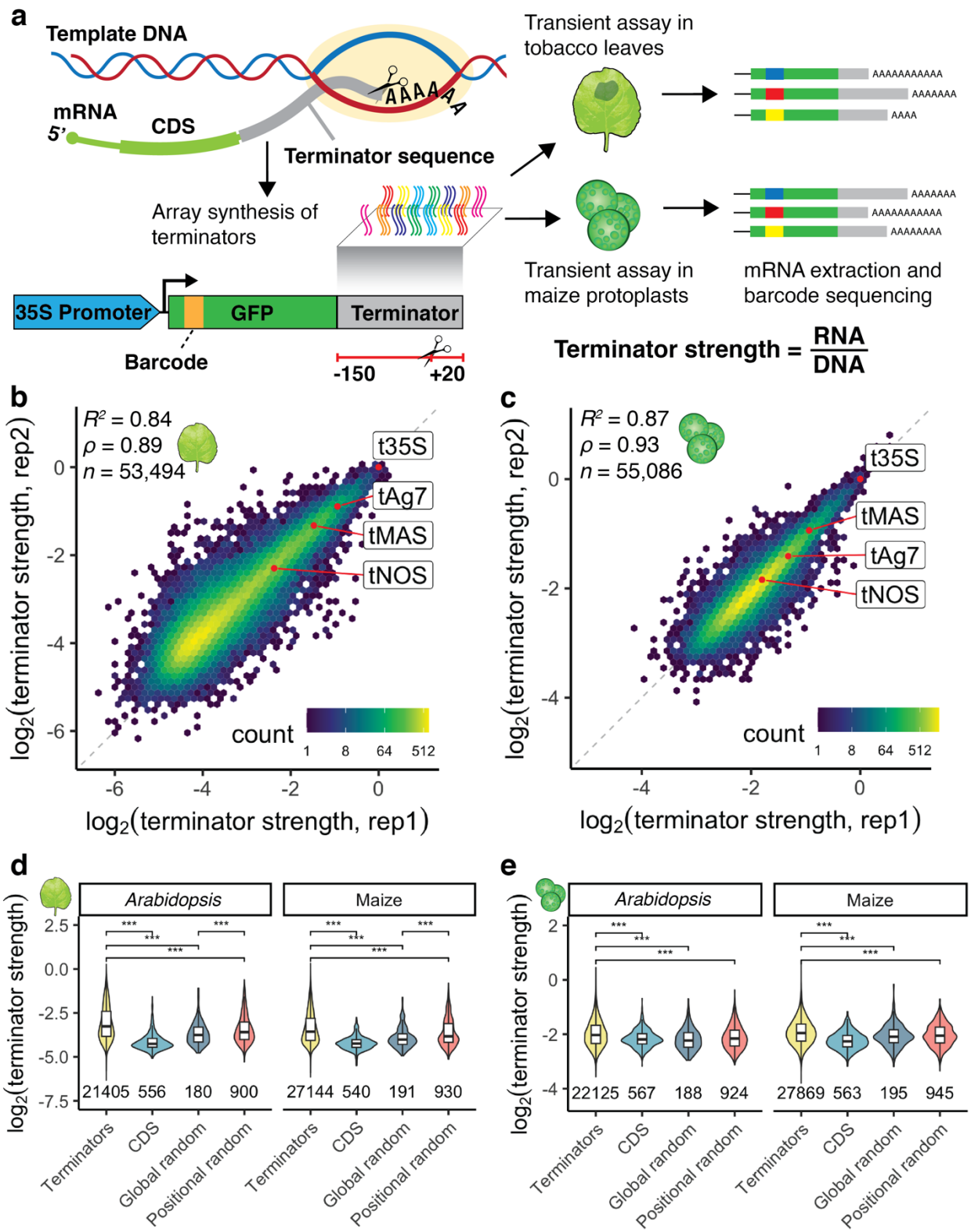

Fig. 1 | Plant STARR-seq measures terminator strength in tobacco leaves and maize protoplasts. a Terminator sequences (bases -150 to +20 relative to the cleavage and polyadenylation site) were array-synthesized and cloned downstream of a barcoded GFP

reporter gene driven by the 35S promoter. After transient expression of the plasmid library in tobacco leaves or maize protoplasts, mRNA was extracted for barcode sequencing. We define terminator strength as the enrichment of barcodes in the extracted mRNA over the input DNA normalized to the strength of the 35S terminator. **b, c** Hexbin plots (color represents the count of points in each hexagon) of the correlation between two biological replicates of Plant STARR-seq in tobacco leaves (**b**) or maize protoplasts (**c**). Commonly used terminators are highlighted in red. Pearson's R^2, spearman's ρ, and number (n) of terminators are indicated. **d, e** Violin plots, box plots, and significance levels of terminator strength in tobacco leaves (**d**) or maize protoplasts (**e**) for plant terminators (Terminators) compared to sequences from coding regions (CDS) and randomized sequences with an overall (Global random) or per-position (Positional random) nucleotide frequency similar to an average *Arabidopsis* or maize terminator. Violin plots represent the kernel density distribution and the box plots inside represent the median (center line), upper and lower quartiles and 1.5× the interquartile range (whiskers) for all corresponding terminators. Numbers at the bottom of each violin indicate the number of terminators in each group. Significant differences between two samples were determined by the two-sided Wilcoxon rank-sum test and are indicated: *$p \leq 0.05$, **$p \leq 0.01$, ***$p \leq 0.001$, NS, not significant. Exact p values are listed in Supplementary Table 5.

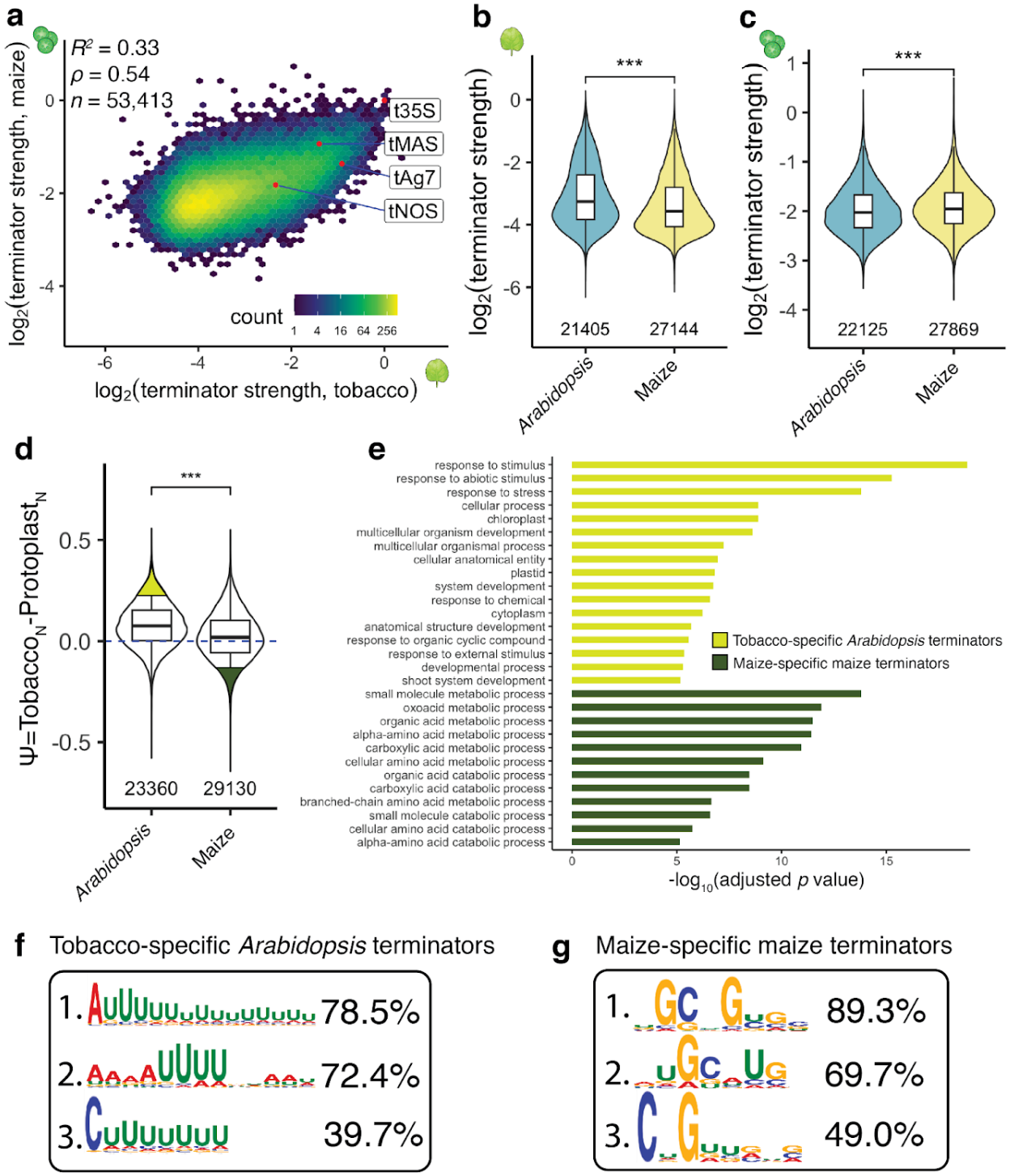

Fig. 2 | Plant terminator strength is species-specific. a Hexbin plot comparing terminator strength in tobacco leaves and maize protoplasts. **b, c** Violin plots of the strength of terminators derived from the indicated species in tobacco leaves (**b**) or maize protoplasts (**c**). **d** Violin plot of Ψ, the difference between normalized (0, weakest; 1, strongest) $\log_2$(terminator strength) in tobacco leaves (Tobacco$_N$) and maize protoplasts (Protoplasts$_N$). Terminators are grouped by

their species of origin. The top 10% of *Arabidopsis* terminators with highest Ψ values (tobacco-specific terminators) and the top 10% of maize terminator with the lowest Ψ values (maize-specific terminators) are highlighted in yellow and green, respectively. **e** GO terms enriched in genes associated with the tobacco-specific *Arabidopsis* terminators or the maize-specific maize terminators highlighted in **d**. Only GO terms with adjusted *p* value ≤ 0.0001 are shown. The *p* values were determined using the gprofiler2 library in R with gSCS correction for multiple testing. All enriched GO terms and exact *p* values are listed in Supplementary Table 6. **f, g** Top three motifs enriched in tobacco-specific *Arabidopsis* terminators relative to maize-specific maize terminators (**f**) and *vice versa* (**g**). The hexbin plot in **a** and the violin plots, box plots, and significance levels in **b**-**d** are as defined in Fig. 1.

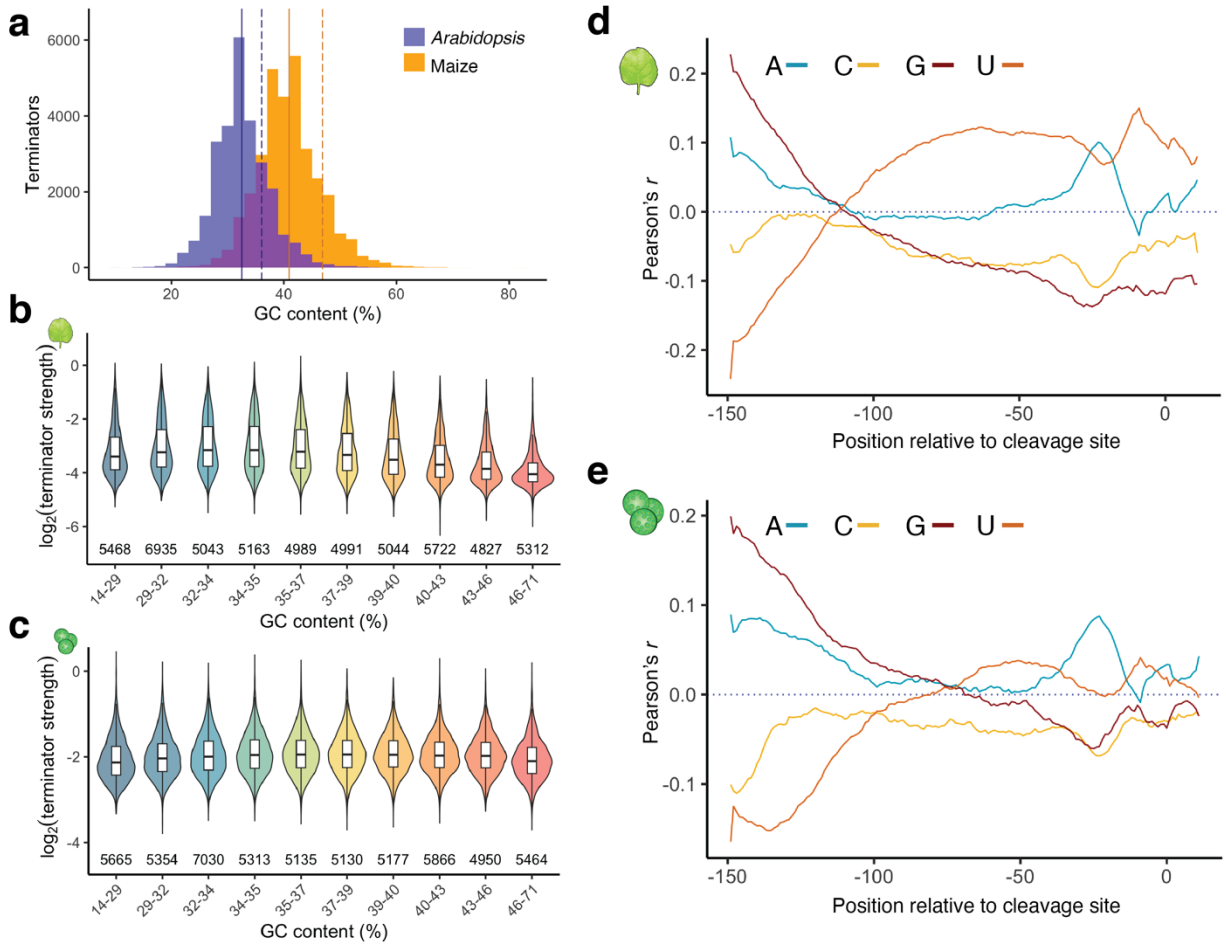

Fig. 3 | Nucleotide composition affects terminator strength in a species- and position-specific manner. a Histogram of terminator GC content. The solid line indicates the mean GC content of terminators (*Arabidopsis* = 32.53%, maize = 40.89%) and the dashed line indicates the GC content of the genome (*Arabidopsis* = 36.06%, maize = 46.86%). **b, c** Violin plots and box plots (as defined in Fig. 1) of terminator strength in tobacco leaves (**b**) or maize protoplasts (**c**). Terminators were binned by GC content to yield groups of approximately the same size. **d, e** Correlation (Pearson's *r*) between terminator strength in tobacco leaves (**d**) or maize protoplasts (**e**) and the A, C, G, or U content of a ten-base window starting at the indicated position in the plant terminators.

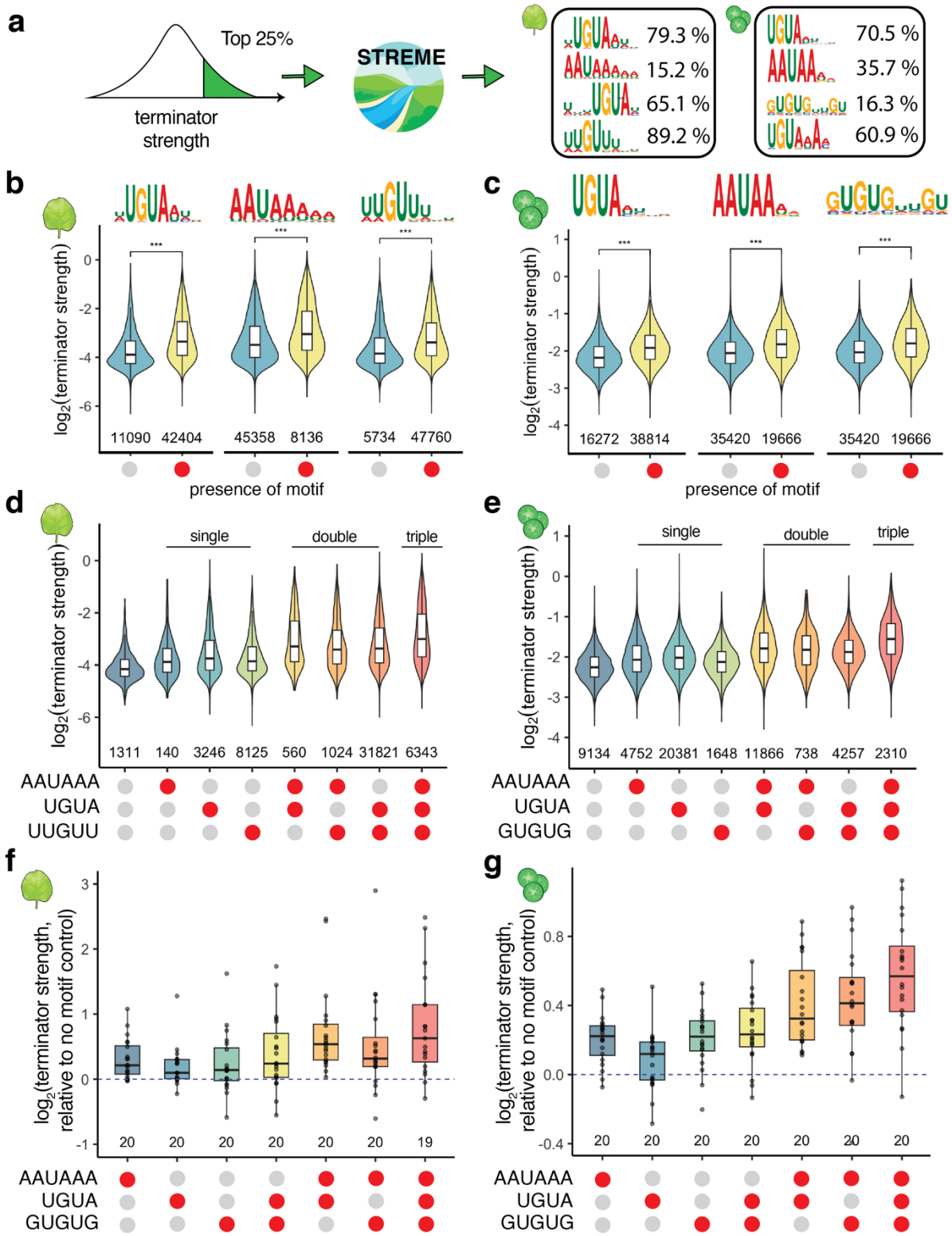

Fig. 4 | Cleavage and polyadenylation motifs increase terminator strength. a Sequence logo plots of the top four motifs enriched in the strongest terminators in tobacco leaves (left) or maize protoplasts (right). For each motif, the percentage of *Arabidopsis* and maize terminators

harboring it is indicated. **b**-**e** Violin plots of terminator strength in tobacco leaves (**b, d**) or maize protoplasts (**c, e**) with or without AAUAAA, UGUA, or U/G-rich motifs individually (**b, c**) or in combination (**d, e**). **f, g** Box plots (centre line, median; box limits, upper and lower quartiles; whiskers, 1.5× interquartile range) and underlying data points for the strength of terminators supplemented with the indicated motifs relative to the corresponding terminator without any motif (set to 0). In **b**-**g**, red circles indicate presence of a motif and gray circle indicate its absence. Violin plots, box plots, and significance levels in **b**-**e** are as defined in Fig. 1.

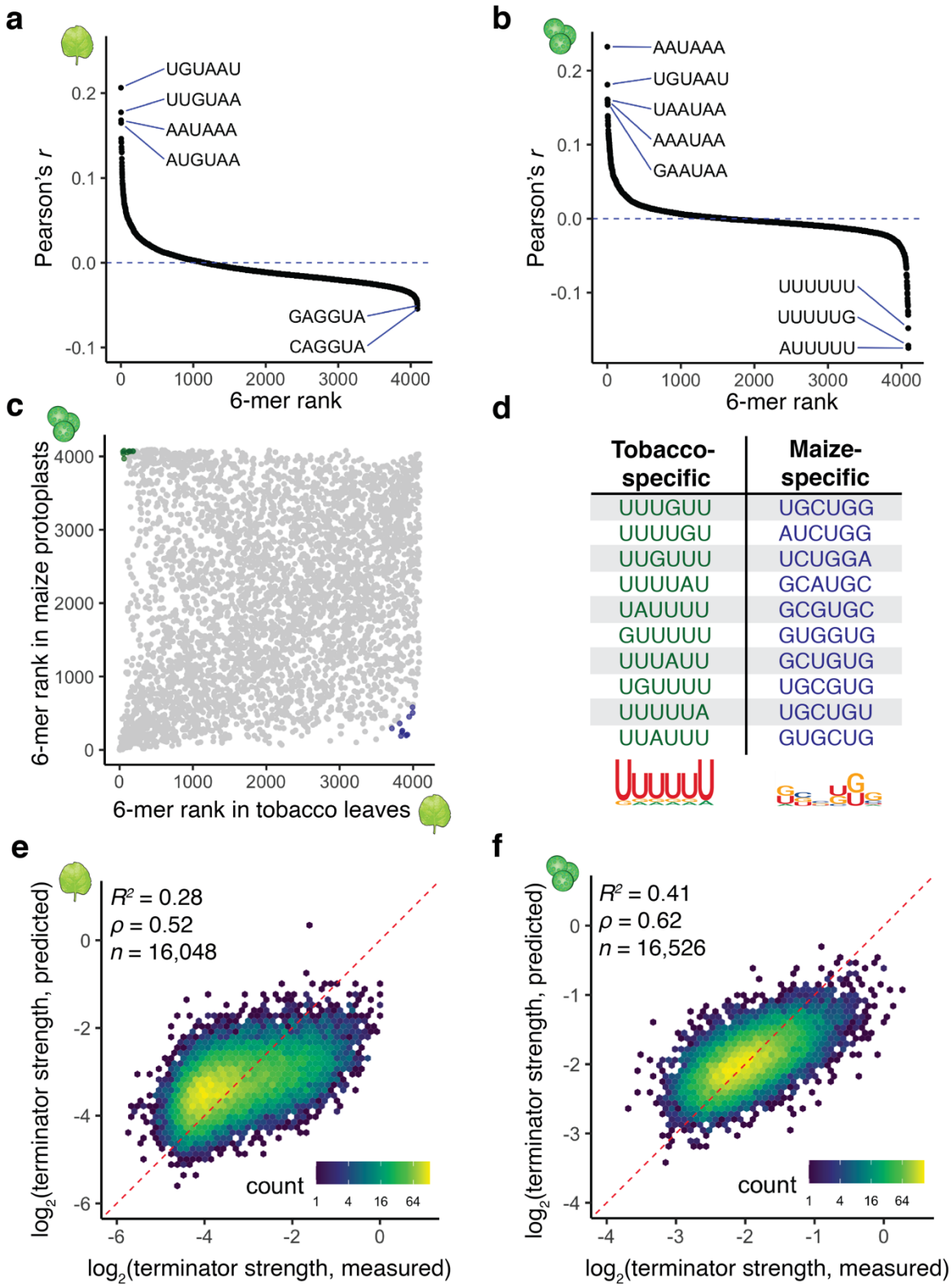

Fig. 5 | K-mers can be used for species-specific terminator strength predictions. a, b Correlation (Pearson's *r*) between terminator strength in tobacco leaves (**a**) or maize protoplasts

(**b**) and how often a given 6-mer is present in the terminators. The horizontal axis displays the 6-mer "rank" based on Pearson's correlation. The sequences of the highest and lowest ranked 6-mers are indicated. **c** Comparison of the 6-mer ranks in tobacco leaves and maize protoplasts. 6-mers highlighted in green and blue had the biggest differences in rank order between the two assay systems. **d** Top 10 tobacco- or maize-specific 6-mers (highlighted in **c**) and sequence logo plots generated from them. **e, f** Hexbin plot (as defined in Fig. 1) of the correlation between terminator strength measured by STARR-seq in tobacco leaves (**e**) or maize protoplasts (**f**) and terminator strength predictions from a lasso regression model based on 6-mer counts. Only the terminators not used for model training are shown (30% of all terminators).

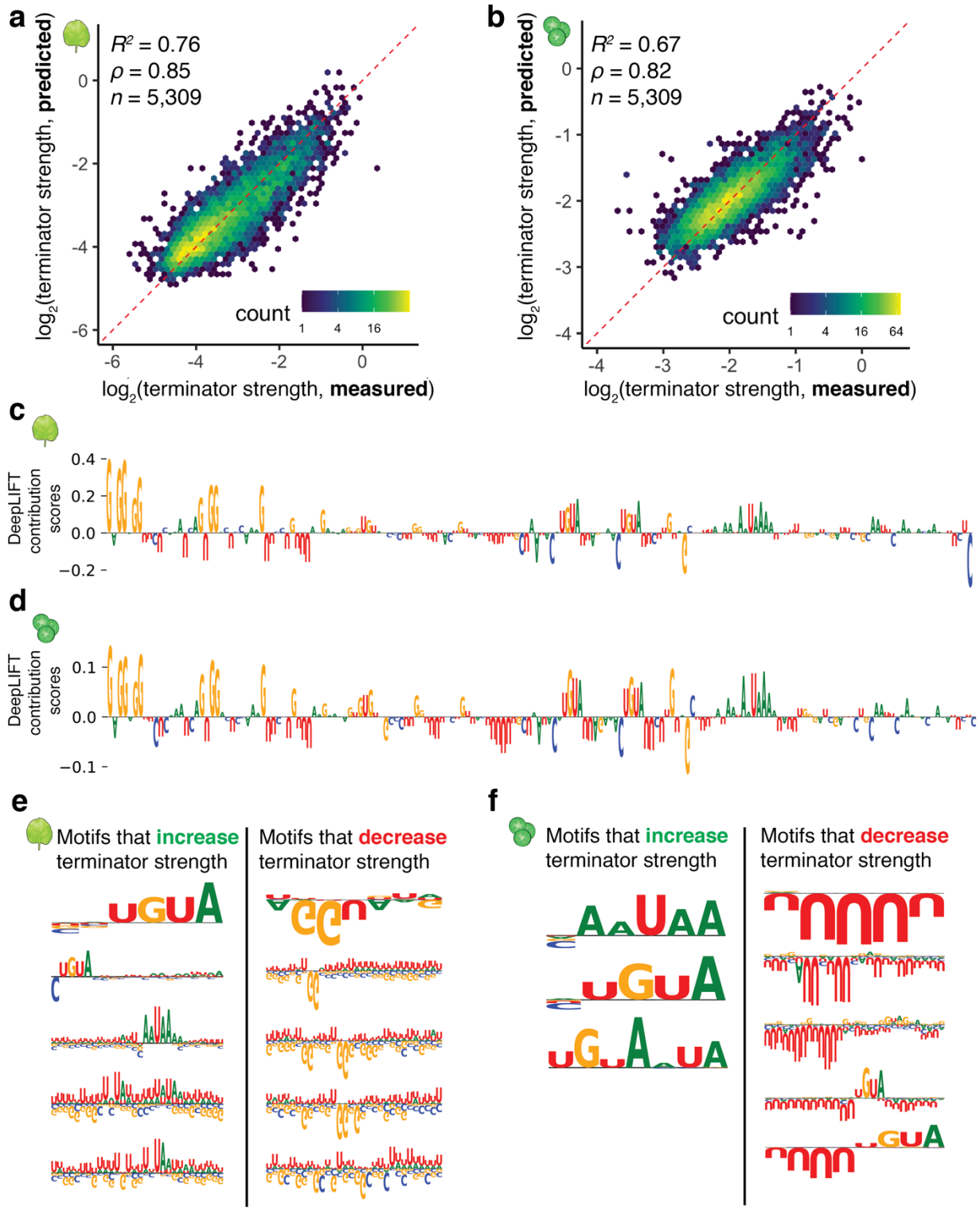

Fig. 6 | A convolutional neural network accurately predicts terminator strength. a, b Hexbin plot (as defined in Fig. 1) of the correlation between terminator strength measured by STARR-seq in tobacco leaves (**a**) or maize protoplasts (**b**) and terminator strength predictions

from a DenseNet convolutional neural network trained on terminator sequences. Only the terminators not used for model training are shown (10% of all terminators). **c, d** DeepLIFT importance scores based on our DenseNet model predictions of terminator strength in tobacco leaves (**c**) or maize protoplasts (**d**). The terminator of AT1G31180 is shown as an example. **e, f** Motifs identified by TF-MoDISco that positively or negatively contribute to the DenseNet model predictions of terminator strength in tobacco leaves (**e**) or maize protoplasts (**f**).

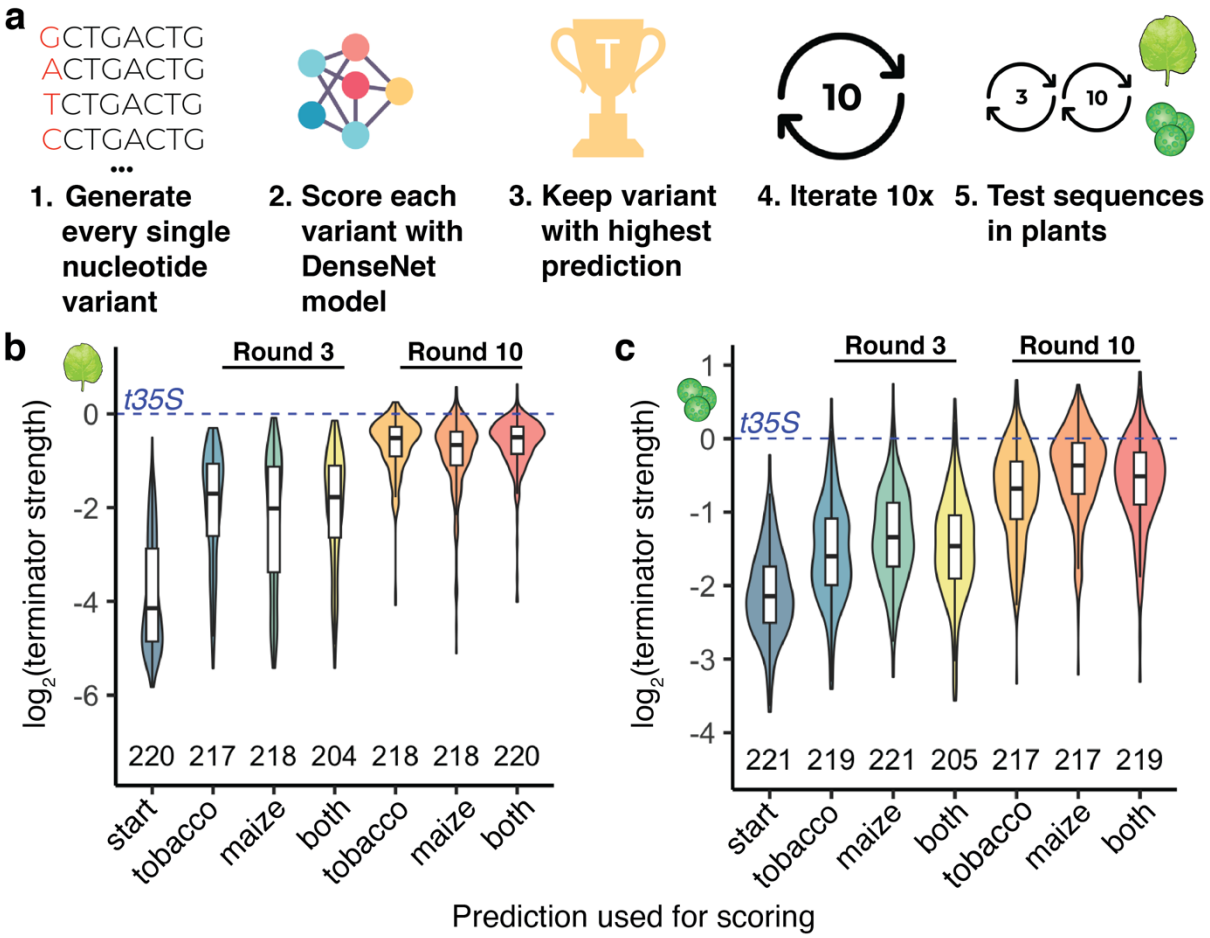

Fig. 7 | *In silico* evolution of plant terminators. a Scheme of the *in silico* evolution. **b, c** Violin plots, box plots, and significance levels (as defined in Fig. 1) of terminator strength measured in tobacco leaves (**b**) or maize protoplasts (**c**) for unmodified terminators (start) and terminators after three or ten rounds of *in silico* evolution. The DenseNet model prediction for tobacco leaves (tobacco) or maize protoplasts (maize), or the sum of both predictions (both) was used as a score during *in silico* evolution. The dashed blue line indicates the strength of the 35S terminator (*t35S*).

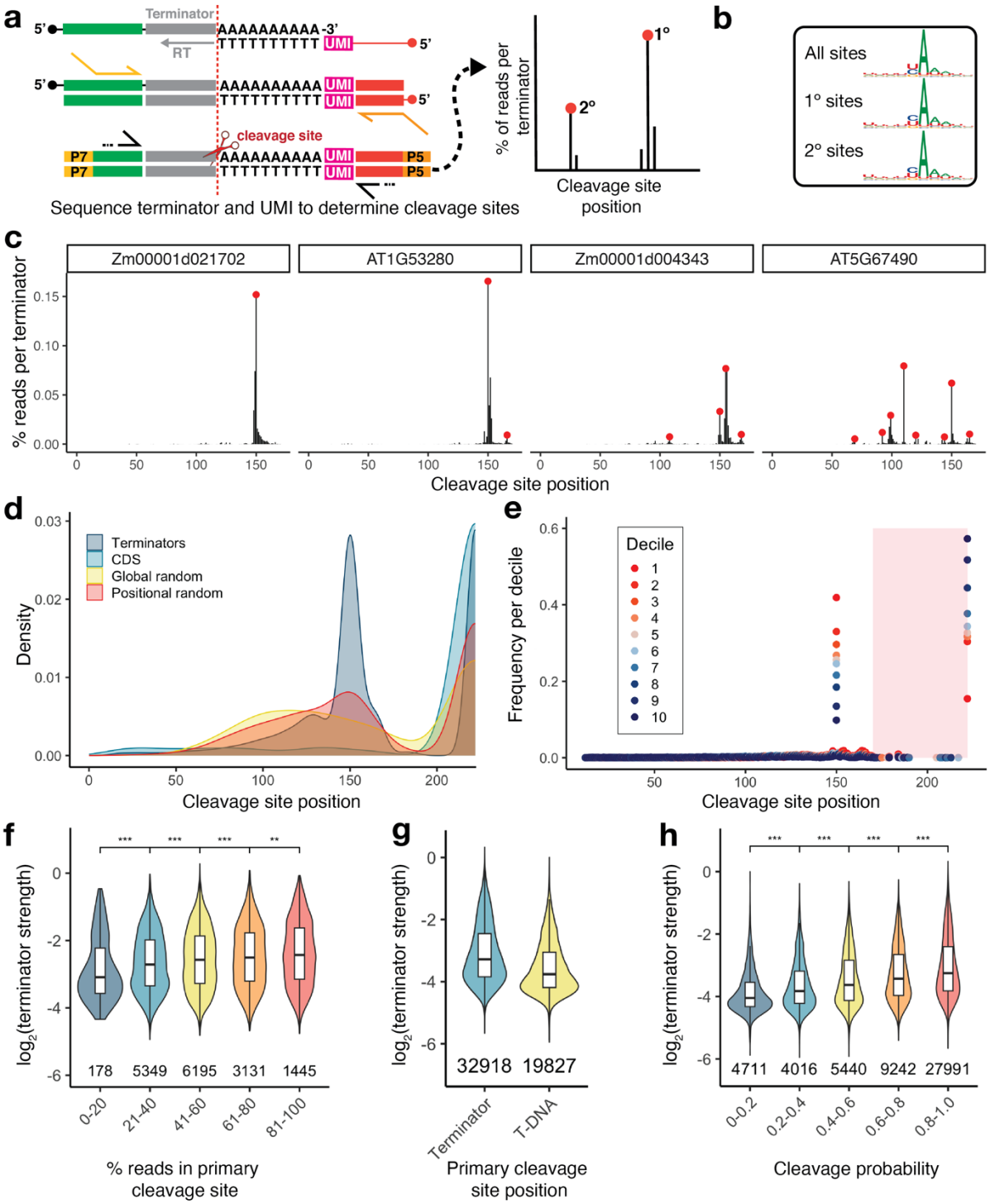

Fig. 8 | Polyadenylation and cleavage affect terminator strength. a Polyadenylation and cleavage sites for terminators in tobacco leaves were determined by 3' end sequencing. Using an oligo-dT primer with a unique molecular identifier (UMI), cDNA was generated from polyadenylated terminators. The cDNA was subjected to paired-end sequencing of the terminator and UMI. Cleavage sites were defined as local maxima in a histogram of terminator read length after trimming of the poly-A tail. **b** Sequence logo plots generated from the 10 bp

window around all cleavage sites (All sites), all primary sites (1° sites), or all secondary sites (2° sites). **c** Histograms of cleavage site position for four representative terminators. Red dots denote primary and alternative cleavage sites. **d** Kernel density distribution of the primary cleavage site position for plant terminators (Terminators), sequences from coding regions (CDS), and randomized sequences with an overall (Global random) or per-position (Positional random) nucleotide frequency similar to an average *Arabidopsis* or maize terminator. **e** Histogram of the primary cleavage site position for terminators grouped into deciles based on terminator strength in tobacco leaves (decile 1 contains the strongest 10% of the terminators and decile 10 the weakest 10%). Each decile contains approximately 5,300 terminators. The shaded red area corresponds to cleavage in the T-DNA backbone (*i.e.* downstream of the terminator sequence). **f** Violin plots of terminator strength. Terminators were grouped by the percentage of reads that coincide with the primary cleavage site. **g** Violin plots of the strength of terminators with a primary cleavage site within the terminator or in the T-DNA. **h** Violin plots of terminator strength for terminators grouped by cleavage probability (percent of unique reads showing cleavage within the terminator sequence). Violin plots, box plots, and significance levels in **f**-**h** are as defined in Fig. 1.

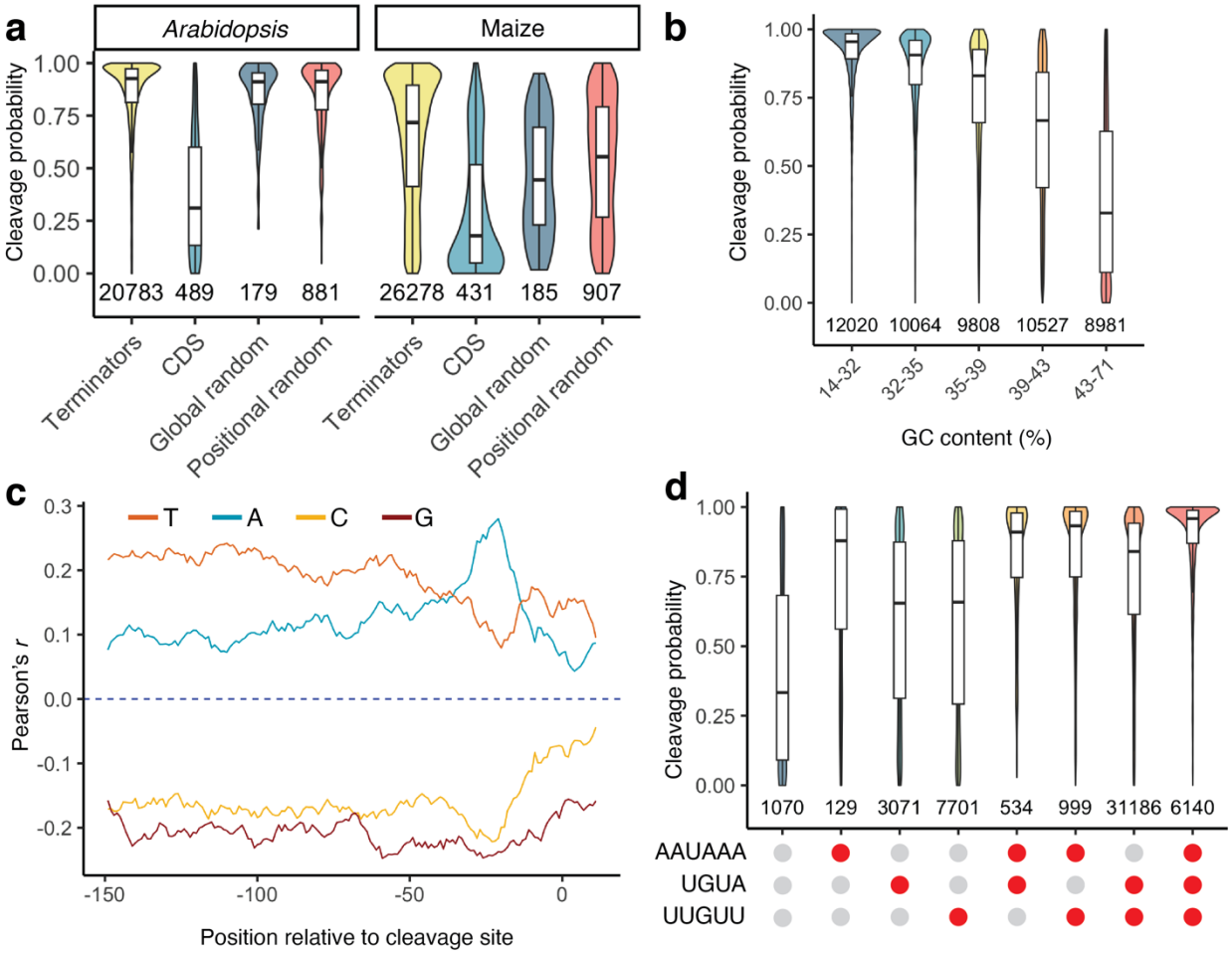

Fig. 9 | GC content and polyadenylation motifs influence cleavage probability. a Violin plots of cleavage probability (percent of unique reads showing cleavage within the terminator sequence) for plant terminators (Terminators) compared to sequences from coding regions (CDS) and randomized sequences with an overall (Global random) or per-position (Positional random) nucleotide frequency similar to an average *Arabidopsis* or maize terminator. **b** Violin plots of cleavage probability. Terminators were binned by GC content to yield groups of approximately the same size. **c** Correlation (Pearson's *r*) between cleavage probability and the A, C, G, or U content of a ten-base window starting at the indicated position in the terminators. **d** Violin plots of cleavage probability for terminators with (red dot) or without (gray dot) the indicated motifs. Violin plots, box plots, and significance levels in **a**, **b**, and **d** are as defined in Fig. 1.

Table 1 | Terminator polyadenylation and cleavage statistics.

Terminator group	**Cleavage site at position 150 ± 5 bp**	**Primary cleavage site at position 150 ± 5 bp**	**Multiple cleavage sites**	**Strong secondary cleavage site (≥ 30% of reads)**	**Cleavage in T-DNA backbone only**
All terminators *n* = 54,825	33,700 (61%)	17,986 (32%)	37,301 (68%)	7,393 (13%)	9,525 (17%)
Arabidopsis terminators *n* = 22,587	15,331 (68%)	8,826 (39%)	16,827 (74%)	4,421 (20%)	1,082 (5%)
Maize terminators *n* = 27,733	16,931 (61%)	8,540 (31%)	18,008 (65%)	2,474 (9%)	6,879 (25%)
CDS *n* = 936	36 (4%)	6 (1%)	234 (25%)	17 (2%)	663 (71%)
Global random sequences *n* = 381	68 (18%)	15 (4%)	227 (60%)	53 (14%)	107 (28.1%)
Positional random terminators *n* = 1,865	773 (41)%	285 (15%)	1,250 (67%)	266 (14%)	388 (21%)

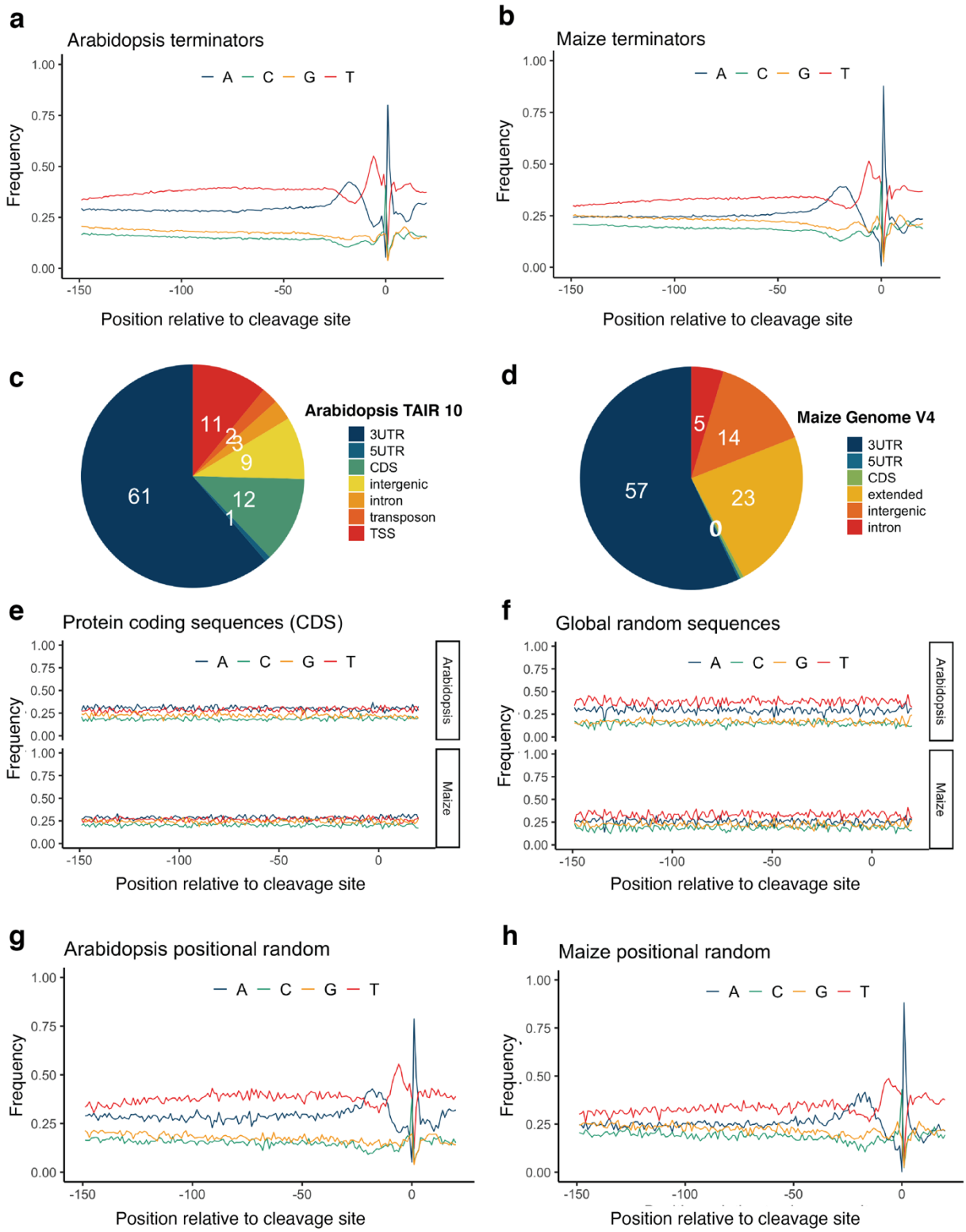

Supplementary Fig. 1 | Nucleotide composition for terminators in our library. a, b Per-position nucleotide frequencies of *Arabidopsis* (**a**) or maize (**b**) terminators. **c, d** Pie charts showing the distribution of the cleavage site location (annotated according to the *Arabidopsis*

TAIR10 and the maize B73v4 genome annotations) for the terminators from *Arabidopsis* (**c**) or maize (**d**) in our library. **e** Per-position nucleotide frequencies for controls derived from coding sequences (CDS) in *Arabidopsis* or maize. **f** Per-position nucleotide frequencies of randomized sequences with an overall (Global random) nucleotide composition similar to average *Arabidopsis* or maize terminator. **g, h** Per-position nucleotide frequencies for randomized sequences with a per-position (Positional random) nucleotide composition similar to an average *Arabidopsis* (**g**) or maize (**h**) terminator.

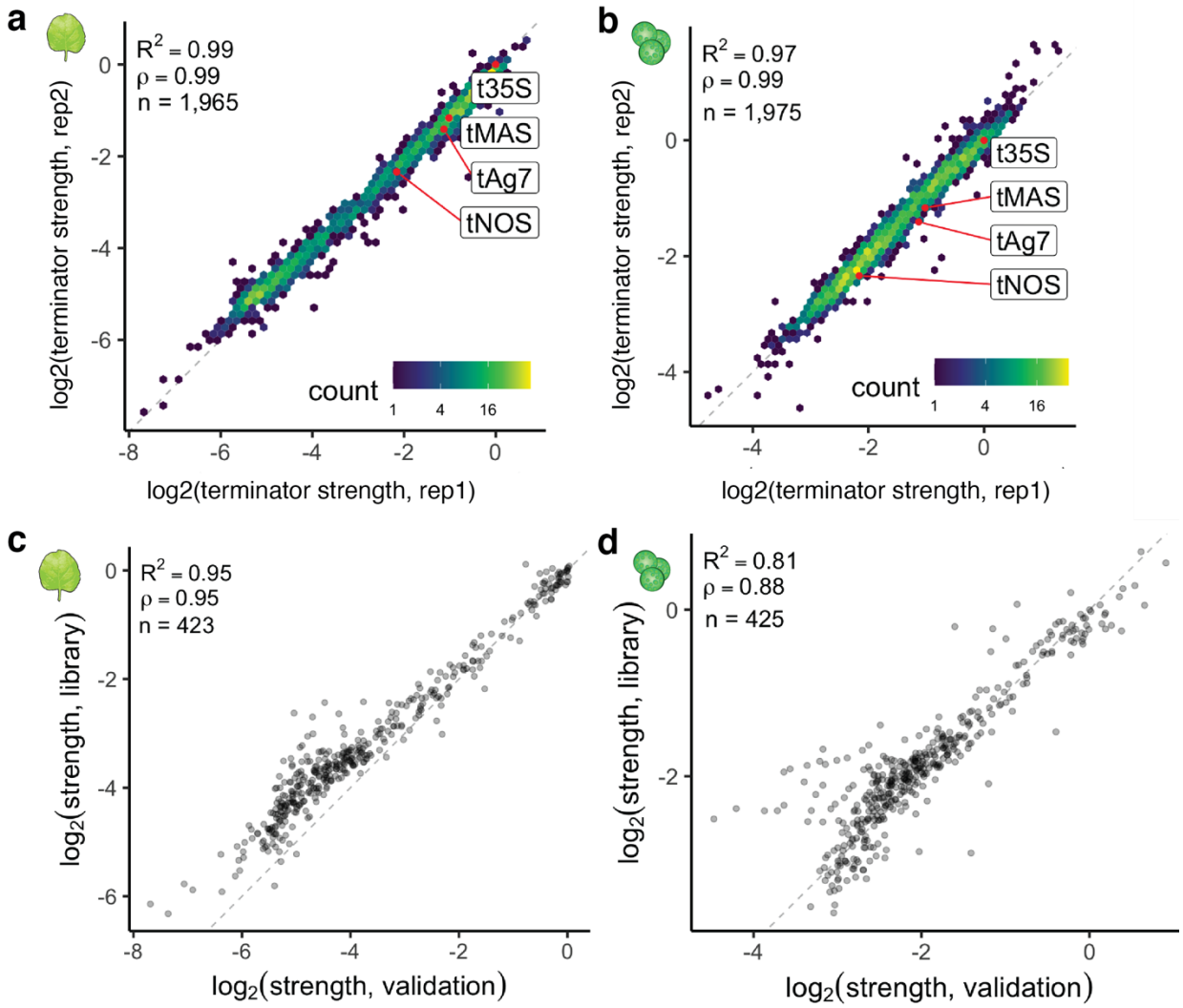

Supplementary Fig. 2 | Plant STARR-seq yields highly reproducible results across libraries. a, b Hexbin plots (as defined in Fig. 1) of the correlation between two biological replicates of Plant STARR-seq with the validation library in tobacco leaves (**a**) or maize protoplasts (**b**). Commonly used terminators are highlighted in red. **c, d** Correlation between terminator strength as measured in the large-scale library and the validation library in tobacco leaves (**c**) or maize protoplasts (**d**). Pearson's R^2, spearman's ρ, and number (n) of terminators are indicated in all plots.

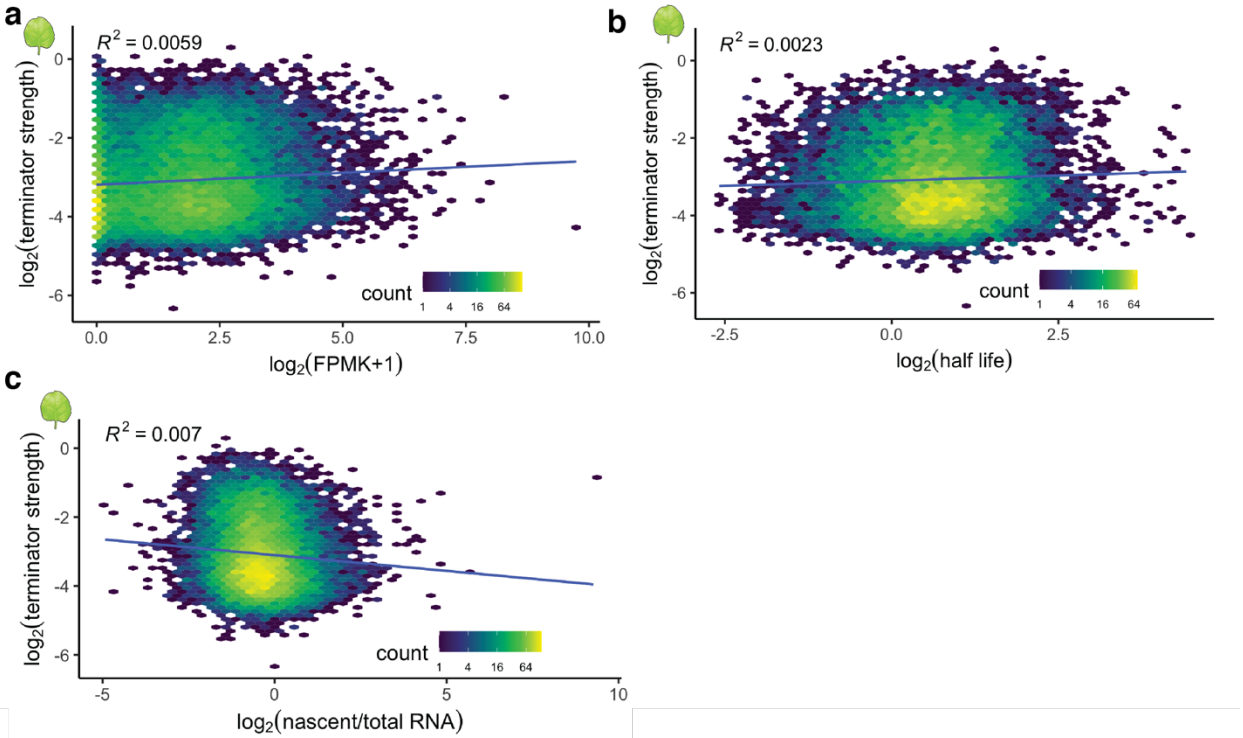

Supplementary Fig. 3 | Terminator strength is not correlated to gene expression, mRNA half-life, and nascent transcription. Hexbin plots (as defined in Fig. 1) of the correlation between the strength of *Arabidopsis* terminators and the expression (**a**), mRNA half-life (**b**), or nascent transcription (**c**) of the corresponding genes. Pearson's R^2 is indicated.
See the main text for data sources.

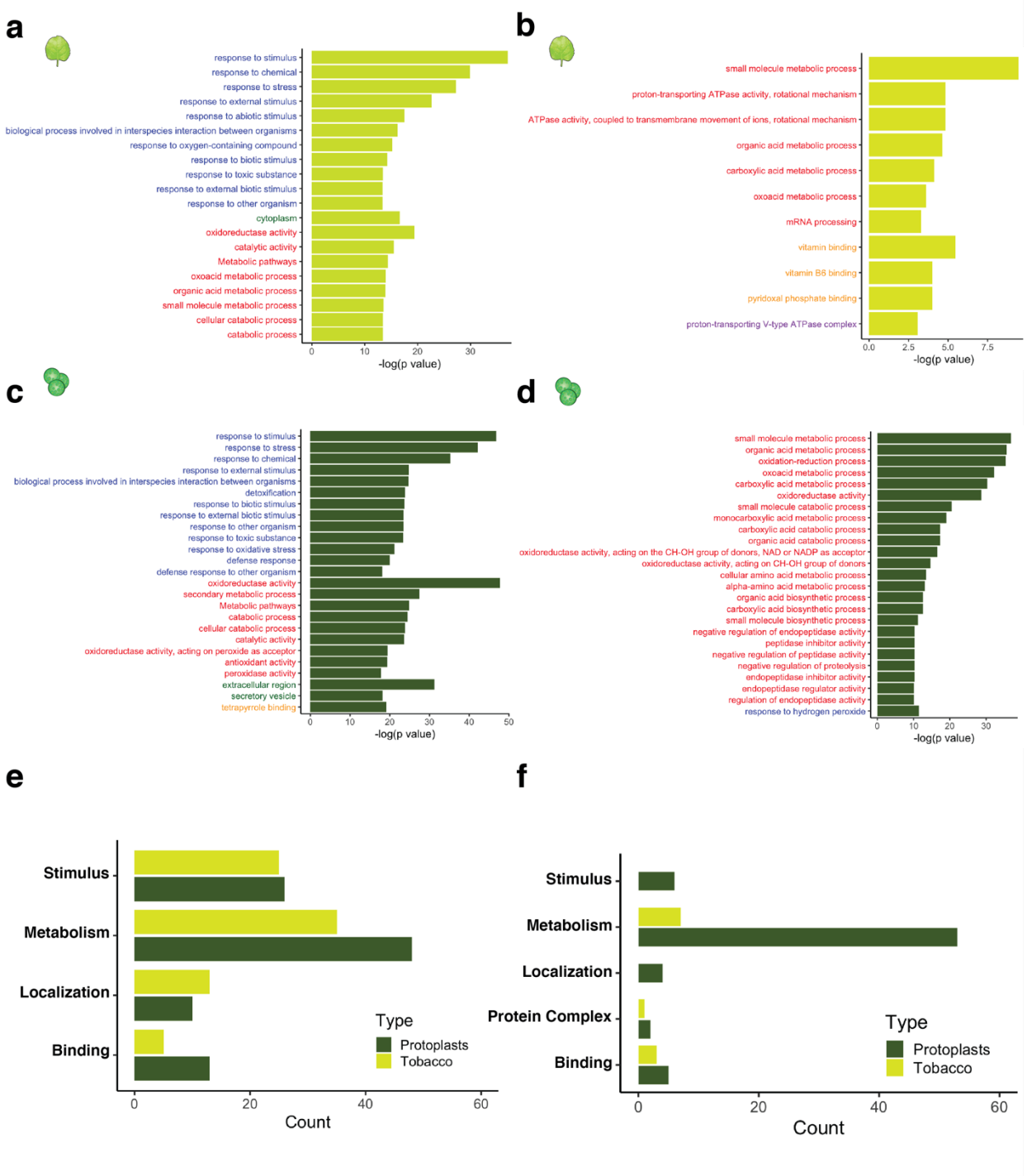

Supplementary Fig. 4 | Metabolic and stimulus-responsive genes frequently use strong terminators. a-d GO terms enriched in genes associated with the top 10% of *Arabidopsis* (**a, c**) or maize (**b, d**) terminators ranked by strength in tobacco leaves (**a, b**) or maize protoplasts (**c, d**). Only the most significant GO terms are shown. The *p* values were determined using the gprofiler2 library in R with gSCS correction for multiple testing. All enriched GO terms and exact

p values are listed in Supplementary Table 6. **e, f** GO terms for *Arabidopsis* (**e**) or maize (**f**) terminators were collapsed into 5 major categories and counted for each assay system.

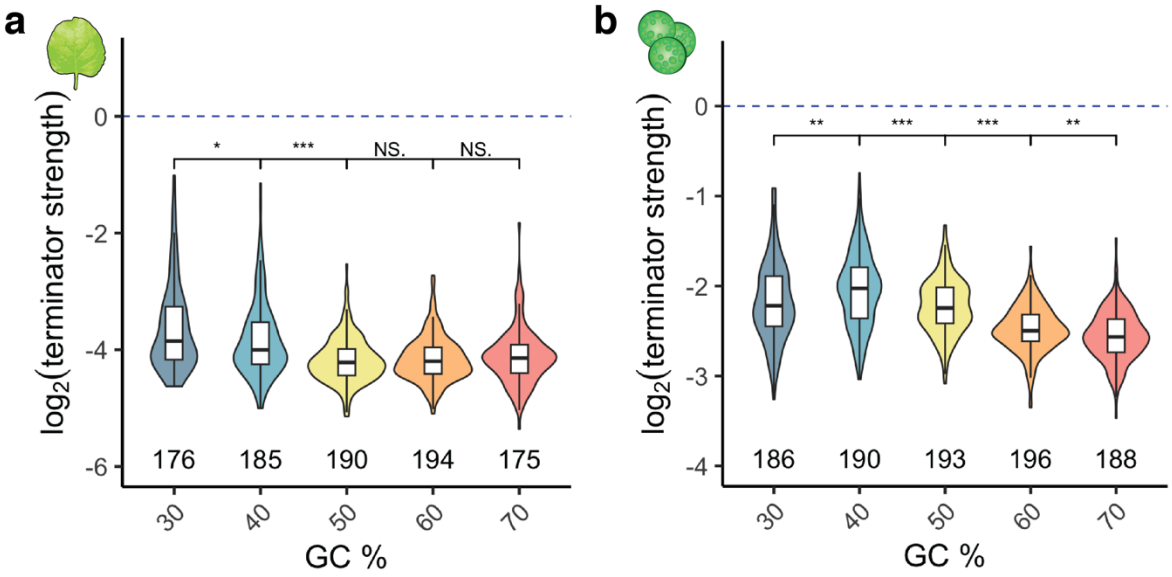

Supplementary Fig. 5 | Optimal GC content for terminators is species-specific. Violin plots, box plots, and significance levels (as defined in Fig. 1) of terminator strength in tobacco leaves (**a**) or maize protoplasts (**b**) for randomized sequences with the indicated GC content.

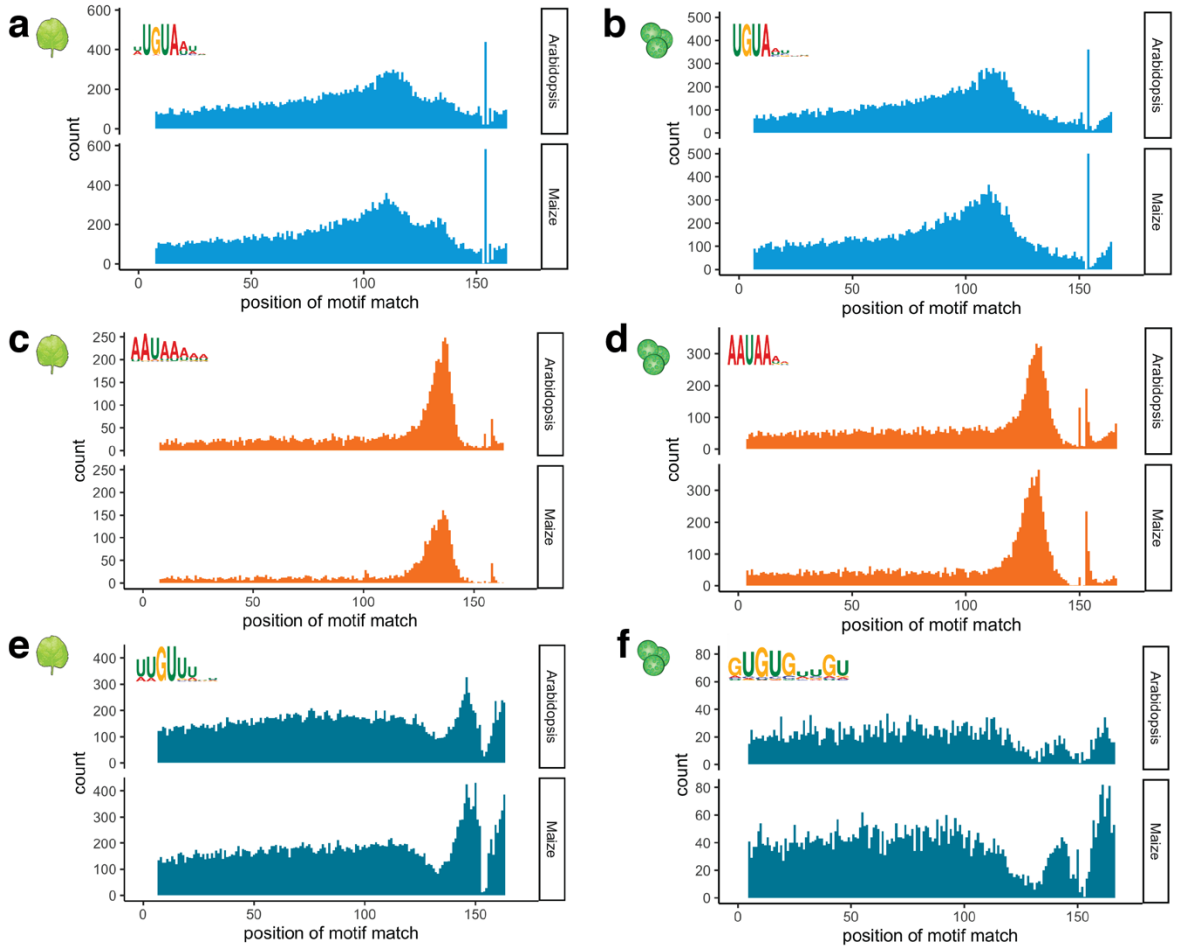

Supplementary Fig. 6 | Polyadenylation motifs show distinct localization profiles. Histograms showing the number of *Arabidopsis* and maize terminators with a UGUA motif (**a, b**), an AAUAAA motif (**c, d**), or a U/G-rich motif (**e, f**) at the indicated position. The motifs were discovered in terminators with high strength in tobacco leaves (**a, c, e**) or maize protoplasts (**b, d, f**).

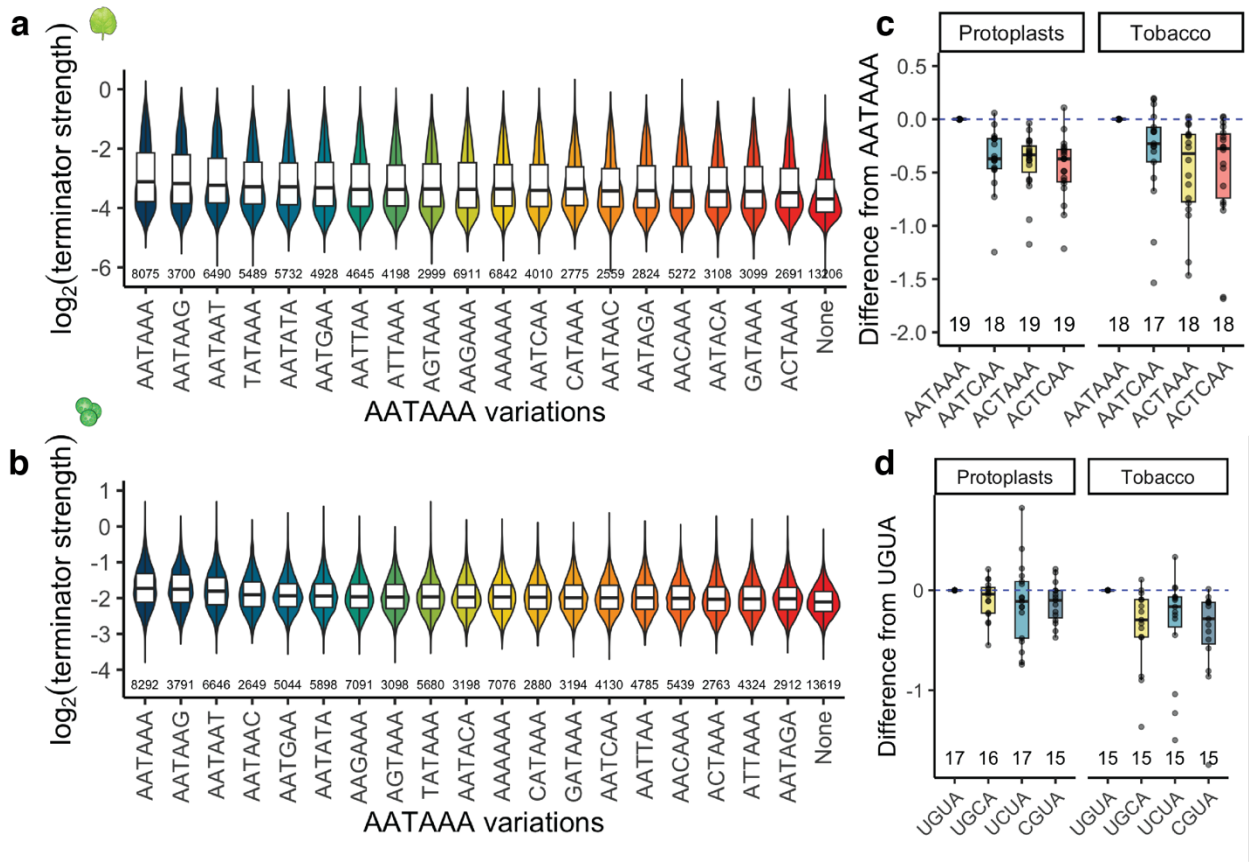

Supplementary Fig. 7 | Cleavage and polyadenylation motifs are sensitive to mutations. **a, b** Violin plots and box plots (as defined in Fig. 1) of terminator strength in tobacco leaves (**a**) or maize protoplasts (**b**) for terminators with the indicated variants of the AAUAAA motif. Terminators without any AAUAAA motif variant (None) are also shown. **c, d** Boxplots (as defined in Fig. 4) of the strength of terminators with the indicated variants of the AAUAAA (**c**) or UGUA (**d**) motif relative to the strength of the corresponding wild type terminator (set to 0).

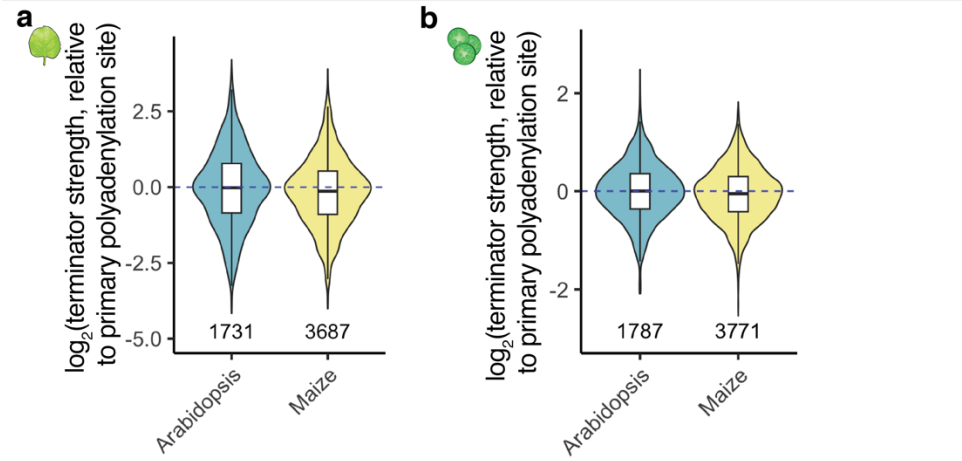

Supplementary Fig. 8 | Terminators derived from primary or secondary polyadenylation sites are indistinguishable by terminator strength. Violin plots and box plots (as defined in Fig. 1) of the terminator strength in tobacco leaves (**a**) or maize protoplasts (**b**) of the experimentally determined secondary polyadenylation site of *Arabidopsis* and maize genes relative to the primary polyadenylation site of the same gene (set to 0).

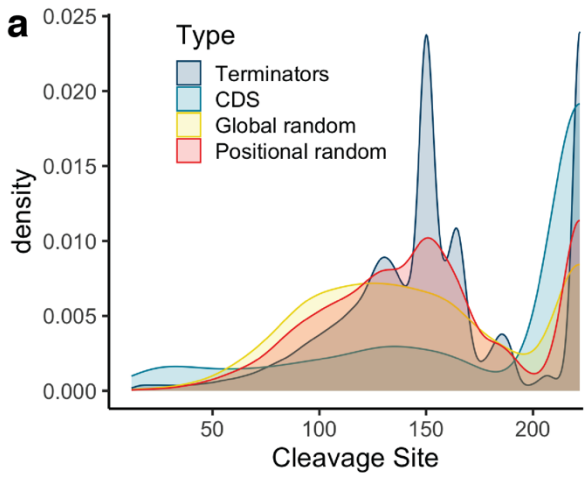

Supplementary Fig. 9 | Cleavage site positions differ between *bona fide* terminators and control sequences. Kernel density distribution of all cleavage site positions for plant terminators (Terminators), sequences from coding regions (CDS), and randomized sequences with an overall (Global random) or per-position (Positional random) nucleotide frequency similar to an average *Arabidopsis* or maize terminator.

Supplementary Table 1 | Terminator library composition.

Type	Count	Description
Arabidopsis terminators (main cleavage site)	22,204	Sequences surrounding main polyadenylation and cleavage site of *Arabidopsis* genes (-150 to +20 relative to cleavage site)
Arabidopsis terminators (secondary cleavage site)	2,325	Sequences surrounding secondary polyadenylation and cleavage site (≥30% of total reads) of *Arabidopsis* genes (-150 to +20 relative to cleavage site)
Maize terminators (main cleavage site)	25,685	Sequences surrounding main polyadenylation and cleavage site of maize genes (-150 to +20 relative to cleavage site)
Maize terminators (secondary cleavage site)	4,407	Sequences surrounding secondary polyadenylation and cleavage site (≥30% of total reads) of maize genes (-150 to +20 relative to cleavage site)
CDS	1,178	Coding sequences (170 bp) with similar overall GC content as *Arabidopsis* or maize terminators (589 from each species)
Fixed GC content	1,000	Randomized sequences (170 bp) with a GC content of: 30%, 40%, 50%, 60%, or 70% (200 each)
Global random sequences	400	Randomized sequences (170 bp) with overall nucleotide frequency similar to an average *Arabidopsis* or maize terminator (200 per species)
Positional random terminators	2,000	Randomized sequences (170 bp) with per-position nucleotide frequency similar to an average *Arabidopsis* or maize terminator (1,000 per species)
Commonly used terminators	4	35S, Ag7, NOS, and MAS terminators

Supplementary Table 4 | Primers and DNA fragments used in this study.

Sequence	Purpose
GTTCCACTTCTGTATAGGAGCCAATTG	linearize pPSup to build pPSt (fwd)
GGAATTCGATATCAAGCTTATCGATACCG	linearize pPSup to build pPSt (rev)
CGGTATCGATAAGCTTGATATCGAATTCCGCTGCCGTCTTCAGTGCCTGCAGGCATAGAAGACCCGTGACGAGACCACAAGGCGCGCCTAGTGGTCTCCTAAGGGAGACGGGATCCTACAGCTAGCCGTCTCGAGGTGTTCCACTTCTGTATAGGAGCCAATTG	Golden Gate cassettes for pPSt (dsDNA fragment)
GGTCGACGAAGACGGGCTG	amplify 35S promoter + Zm00001d041672 5'UTR (fwd)
GAGAGGAAGACGGTCACNNBNNGNNBNNGNNBNNBCATCGGGGAAGGCTGGG	amplify 35S promoter + Zm00001d041672 5'UTR (rev; contains barcode)
GCGCCGTCTCCTAAG<170bp_terminator>AGGTCGAGACGGTGC	terminator oligo pool
GCGCCGTCTCCTAAG	amplify terminator oligo pool (fwd)
GCACCGTCTCGACCT	amplify terminator oligo pool (rev)
CAGGTCGACGGTCTCCGTGAGCAAGGGCGAGGAG	amplify GFP (fwd)
TCCTCTAGAGGTCTCGCTTACTTGTACAGCTCGTCCATGCC	amplify GFP (rev)
AGTTCAGCCACATGGTCCTGCTGGAGTTC	delete central portion of GFP (fwd)
GGACCATGTGGCTGAACTTGTGGCCGTTTA	delete central portion of GFP (rev)
GGACGACGTCGTCTCCTAAGCTCTAGCTAGAGTCGATCGACAAGCTCGAGTTTCTCCATAATAATGTGTGAGTAGTTCCCAGATAAGGGAATTAGGGTTCCTATAGGGTTTCGCTCATGTGTTGAGCATATAAGAAACCCTTAGTATGTATTTGTATTTGTAAAATACTTCTATCAATAAAATTTCTAATTCCTAAAACCAAAATCCAGTACTAAAATCCAGATAGGTCGAGACGACGTCGTAC	template 35S terminator
GGACGACGTCGTCTCCTAAGCTCTAGCTAGAGTCGATCG	amplify 35S terminator (fwd)
GTACGACGTCGTCTCGACCTATCTGGATTTTAGTACTGGATTTTG	amplify 35S terminator (rev)
GGACGACGTCGTCTCCTAAGGATCGTTCAAACATTTGGC	amplify NOS terminator (fwd)
GTACGACGTCGTCTCGACCTGATCTAGTAACATAGATGACACC	amplify NOS terminator (rev)
GGACGACGTCGTCTCCTAAGCTTGGACTCCCATGTTGGCAAAGGCAACCAAACAAACAATGAATGATCCGCTCCTGCATATGGGGCGGTTTGAGTATTTCAACTGCCATTTGGGCTGAATTGTAGACATGCTCCTGTCAGAAATTCCGTGATCTTACTCAATATTCAGTAATCTCGGCCAATATCCTAAATGTGCGTGGCTTTATCTGTCTTTGTATTGTTTCATCAATTCATGTAACGTTTGCTTTTCTTATGAATTTTCAAATAAATTATCAGGTCGAGACGACGTCGTAC	template MAS terminator

GGACGACGTCGTCTCCTAAGCTTGGACTCCCATGTTG	amplify MAS terminator (fwd)
GTACGACGTCGTCTCGACCTGATAATTTATTTGAAAATTCATAAGAA	amplify MAS terminator (rev)
GGACGACGTCGTCTCCTAAGGCTAGCTATATCATCAATTTATGTATTACACATAATATCGCACTCAGTCTTTCATCTACGGCAATGTACCAGCTGATATAATCAGTTATTGAAATATTTCTGAATTTAAACTTGCATCAATAAATTTATGTTTTTGCTTGGACTATAATACCTGACTTGTTATTTTATCAATAAATATTTAAACTATATTTCTTTCAAGATGGGAATTAGGTCGAGACGACGTCGTAC	template Ag7 terminator
GGACGACGTCGTCTCCTAAGGCTAGCTATATCATCAATTTATG	amplify Ag7 terminator (fwd)
GTACGACGTCGTCTCGACCTAATTCCCATCTTGAAAGAAATATAGT	amplify Ag7 terminator (rev)
GAACTTGTGGCCGTTTACG	reverse transcription for barcode sequencing
AATGATACGGCGACCACCGAGATCTACAC<8bp_index2>CCTCGGCCTCCCTGTCC	amplify barcode for NGS (fwd)
CAAGCAGAAGACGGCATACGAGAT<8bp_index1>CACCCCGGTGAACAGCTCC	amplify barcode for NGS (rev)
CCTCGGCCTCCCTGTCCCCAGCCTTCCCCGATG	NGS read 1 primer for barcode sequencing
CACCCCGGTGAACAGCTCCTCGCCCTTGCTCAC	NGS read 2 primer for barcode sequencing
GTGAGCAAGGGCGAGGAGCTGTTCACCGGGGTG	NGS index 1 primer for barcode sequencing
CATCGGGGAAGGCTGGGGACAGGGAGGCCGAGG	NGS index 2 primer for barcode sequencing
ACGACGCTCTTCCGATCTNNNNNNNNTTTTTTTTTTTTTTTTTTTTTTTTTTTVN	reverse transcription primer for 3’ end sequencing
AATGATACGGCGACCACCGAGATCTACAC<8bp_index2>GGATCACTCACGGCATGGAC	amplify terminator 3’ end (fwd)
CAAGCAGAAGACGGCATACGAGAT<8bp_index1>ACACTCTTTCCCTACACGACGCTCTTCCGATCT	amplify terminator 3’ end (rev)
GGATCACTCACGGCATGGACGAGCTGTACAAGTAAG	NGS read 1 primer for 3’ end sequencing
Illumina TruSeq read 1 primer (ACACTCTTTCCCTACACGACGCTCTTCCGATCT)	NGS read 2 primer for 3’ end sequencing
Illumina TruSeq index 2 primer (AGATCGGAAGAGCGTCGTGTAGGGAAAGAGTGT)	NGS index 1 primer for 3’ end sequencing
CTTACTTGTACAGCTCGTCCATGCCGTGAGTGATCC	NGS index 2 primer for 3’ end sequencing
AATGATACGGCGACCACCGAGATCTACAC<8bp_index2>CCTCGGCCTCCCTGTCC	amplify terminator library for subassembly (fwd)
CAAGCAGAAGACGGCATACGAGATGCAACCAAGATGCATGTTGTCATCATTGGCTCC	amplify terminator library for subassembly (rev)

GGATCACTCACGGCATGGACGAGCTGTACAAGTAAG	NGS read 1 primer for subassembly sequencing
GATGCATGTTGTCATCATTGGCTCCTATACAGAAGTGGAACACCT	NGS read 2 primer for subassembly sequencing
CCTCGGCCTCCCTGTCCCCAGCCTTCCCCGATG	NGS index 1 primer for subassembly sequencing
CACCCCGGTGAACAGCTCCTCGCCCTTGCTCAC	NGS index 2 primer for subassembly sequencing